Ecological Indicators 174 (2025) 113376

Contents lists available at ScienceDirect

Ecological Indicators

journal homepage: www.elsevier.com/locate/ecolind

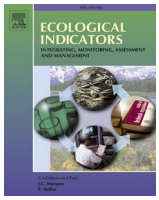

Source-specific probabilistic health risk assessment of potentially toxic elements in soils from a mining area using Monte Carlo simulation: A case study from southwestern Ghana

Raymond Webrah Kazapoe [a], Daniel Kwayisi [b,c,*], Seidu Alidu [d], Samuel Dzidefo Sagoe [e], Ebenezer Ebo Yahans Amuah [f], Obed Fiifi Fynn [g], Pearl Ama Ndo [h], Portia Annabelle Opoku [i], Bawa Naziru [j]

[a] Department of Geological Engineering, University for Development Studies, Nyankpala, Ghana
[b] Department of Geology, University of Johannesburg, Auckland Park Kingsway Campus, South Africa
[c] Department of Earth Science, University of Ghana, Legon-Accra, Ghana
[d] Ghana Geological Survey Authority, P.O. Box M80, Accra, Ghana
[e] Department of Environment and Sustainability Sciences, University for Development Studies, Ghana
[f] Department of Civil Engineering, Takoradi Technical University, P. O. Box 256, Takoradi, Ghana
[g] Department of Geological Sciences, University of Energy and Renewable Resources, Sunyani, Ghana
[h] Pan African University Life and Earth Sciences Institute (PAULESI), University of Ibadan, P. O. Box P.M.B, Ibadan, Nigeria
[i] College of Hydrology and Water Resources. Hohai University, Nanjing 210098, China
[j] Department of Earth Science, University for Development Studies, Navrongo, Ghana

ARTICLE INFO

Keywords:
Gold mining
Pollution
Geochemistry
Self Organising Maps
Heavy Metals

ABSTRACT

This study evaluates the impact of mining on soil contamination by conducting a source-specific probabilistic health risk assessment of Potentially Toxic Elements (PTEs) in Southwestern Ghana. Using an Energy-Dispersive X-ray Fluorescence (ED-XRF) spectrometer, 720 soil samples were analyzed for their elemental concentrations. The samples were obtained in 2024 from the B-horizon to provide better accuracy in detecting actual contamination levels linked to illegal mining activities. The PTEs with the highest frequency above their Upper Continental Crustal Averages (UCC) were As(100 %), Ba(13 %), Cr(5.8 %), Pb(2.7 %), Co(2 %), V(2 %), Cu(0.4 %) and Zn(0.4 %). Correlation Coefficient, Self-Organizing Maps (SOM) and Principal Component Analysis (PCA) identified three groups of PTEs, which are geochemically linked elements (Ba, Cr, Cu, Ni, V), anthropogenically influenced As, and a group with low correlations (Co, Pb). Results indicate that anthropogenic activities, such as gold extraction, partly drive As distribution. Geoaccumulation and Pollution Indices reveal varying levels of pollution in As, Cr, and Pb. Health risk assessments, using deterministic and probabilistic methods, found that while non-carcinogenic risks were within safe limits for adults (Hazard Index [HI] < 1), children faced higher risks (HI > 1) for As, Cr, Co, and V. Carcinogenic risks for both groups were within the acceptable threshold (10^{-4}–10^{-6}), with children at greater risk. Ingestion was identified as the primary exposure pathway. The study highlights the higher susceptibility of children to PTE pollution, emphasising the need for interventions to mitigate risks from PTEs.

1. Introduction

Although mining contributes significantly to the economic development of Ghana, it is also associated with serious environmental and public health risks (Kazapoe et al, 2023). A critical issues of concern associated with this is the contamination of soil and water resources with Potentially Toxic Elements (PTEs) such as arsenic, cadmium, and lead, which are released in the course of the mining process (Agyeman et al, 2021). There is a risk of these contaminants entering the food chain, water sources, and air if left uninhibited, bringing about serious health risks for nearby communities (Emmanuel et al., 2018). Like many regions in Ghana, Southeastern Ghana is heavily impacted by both

* Corresponding author.
E-mail address: dkwayisi@ug.edu.gh (D. Kwayisi).

https://doi.org/10.1016/j.ecolind.2025.113376
Received 7 January 2025; Received in revised form 10 March 2025; Accepted 17 March 2025
Available online 11 April 2025

artisanal and large-scale mining, highlighting this problem (Gbedzi et al, 2022). Understanding the degree of contamination and the health implications that come with it is integral for the protection of vulnerable populations and the safeguarding of the environment.

There are myriads of ways through which PTEs are introduced into the environment. These processes, both natural and anthropogenic, often include activities like mining, industrial emissions, and agricultural practices (Wani et al, 2023; Zhang et al, 2024). Exposure to these contaminants by humans happens through three primary pathways, ingestion, dermal, and inhalation. Exposure through ingestion can occur through the consumption of contaminated crops, dermal exposure can occur through direct skin contact with contaminated soils, and exposure through inhalation can occur through breathing in contaminated soil particles (Opoku et al., 2020). The health effects associated with PTEs range from gastrointestinal issues to chronic conditions including neurological damage and cancer (McKone and Daniels, 1991).

The value of merging environmental management and policy in mitigating the impacts of contamination from mining related activities cannot be overstated. Effective management involves understanding the pathways through which PTEs are released and distributed in the environment. Policies must be designed based on robust scientific evidence to target key sources of pollution, prioritize remediation and protect vulnerable communities. The absence of comprehensive assessments and policies designed specifically to combat unique problems leads to disorganized and ineffective mitigation efforts, abandoning communities and exposing them to long-term health and environmental risks.

Past literature has extensively documented the presence of PTEs in mining regions, with a primary focus on quantifying contamination levels or on assessing health risks with limited integration of these two aspects (Mensah et al., 2015a; Banchirigah, 2008). However, these pollutants are highly variable, strongly influenced by natural factors such as elevation, soil properties, and local environment, resulting in pronounced differences in the region (Kowalska et al., 2022). Geostatistical and multivariate statistic spatial mapping techniques are useful tools for source identification and investigation of relationships among pollutants (Hou et al., 2017; Kazapoe et al., 2024). Although employed with utility, these approaches primarily emphasize the spatial distributions, leaving out some subtle variations and complicated heterogeneities in pollution behaviour (Amuah et al., 2022).

Furthermore, most previous investigations of health risks as a consequence of these contaminants have been based on deterministic frameworks, in which a single point measurement is used to make an estimate of environmental risk. These methods are widely used, but their uncertainties are compounded as they do not properly account for the dynamism of pollutant concentrations, sources, or the dynamics in ecosystems themselves (Dong et al., 2015). These are restrictions that point to the need for more robust methodologies to provide greater and more accurate risk assessment.

In response to these problems, this research integrates multivariate, deterministic and probabilistic approaches, including Monte Carlo simulation, to provide robust assessments of PTEs in southwestern Ghana which is largely a mining-endemic area. Most notably, this combined strategy not only minimizes uncertainties, but also helps establish a more reliable basis for risk assessment of the environmental and human health impacts associated with spatiotemporal variability. By integrating source apportionment techniques with Monte Carlo simulation, the research seeks to provide actionable insights for environmental management and inform policy recommendations.

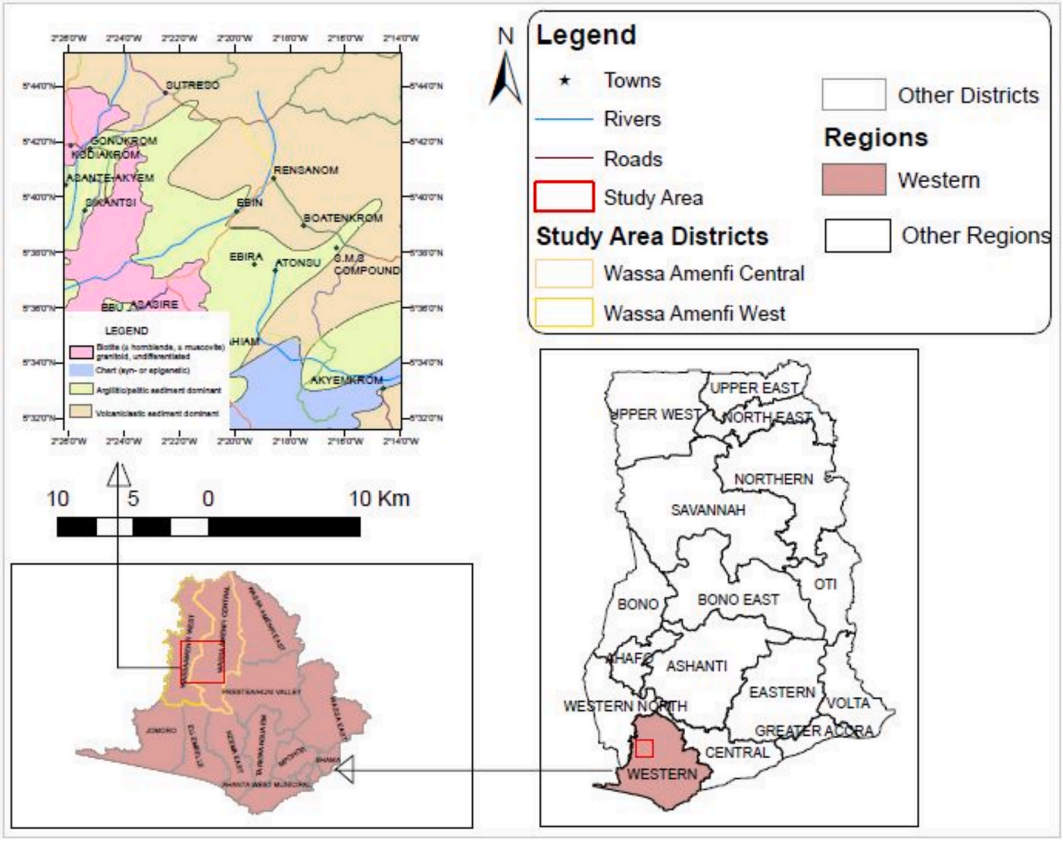

Fig. 1. Location map of the Wassa Amenfi West and Central Districts.

2. Methods

2.1. Area of study

The study area, which is located in the Western Region of Ghana, consists of the Wassa Amenfi Central and Wassa Amenfi West districts (Fig. 1). With a total area size of 1,643 km^2 (634 sq mi), the geographical location is 5°37′59.52″N 2°15′4.32″W (Owusu-Nimo et al., 2018). Gold and cocoa production are the main income sources for its inhabitants (Boakye Dankwah et al., 2024; Enu-Kwesi et al., 2023).

Wassa Amenfi is drained by many streams and rivers that are important to mining and agriculture. The water bodies also serve a huge function in irrigation in the dry seasons to supply the farms (Asare et al., 2019). Unfortunately, illegal mining works, colloquially referred to as 'Galamsey,' have significantly impacted the drainage system, leading to soil erosion and water pollution (Ofori et al., 2024; Wireko-Gyebi et al., 2020). The degradation of these water bodies serves as a significant hazard to the health of local ecosystems and sustainable farming practices (Kuffour et al., 2020; Ofori et al., 2024).

The Wassa Amenfi district generally has clayey and loamy soil types, suitable for cocoa growth. The region's meteorological conditions are ideal boost for soil fertility due to large amounts of rainfall and humidity. Despite this, mining operations have seriously contaminated the soil with heavy metals, creating huge problems for food safety and human health (Afriyie et al., 2023; Gyimah, 2019). These operations negatively affect the quality of the soil close to the mining area and mess up agricultural productivity (Enu-Kwesi et al., 2023).

The Wassa Amenfi District is a demographically heterogeneous population. The population consists of several ethnic groups, of which a large part grows cocoa. According to recent estimates, there are roughly 42,578 cocoa growers in Wassa Amenfi West and 26,500 in Wassa Amenfi Central, emphasising cocoa's importance as the region's principal economic driver (Boakye Dankwah et al., 2024; Enu-Kwesi et al., 2023). Furthermore, agricultural and mining operations, such as pesticide and heavy metal exposure, plague the population with health difficulties (Afriyie et al., 2023; Gyimah, 2019).

The Wassa Amenfi traditional area is primarily composed of rocks from the Paleoproterozoic Birimian terrane, which formed during the Eburnean orogenic events at ca. 2.1 Ga (Kazapoe et al., 2022; 2023; Sakyi et al., 2024). The northern and eastern parts of the study area are underlain by volcaniclastic sediments dated at 2159 ± 4 Ma, Whereas the western and southwestern parts are mainly argillites and pelitic rocks dated at 2139 ± 2 Ma. Chert of 2134 Ma occupies the southeastern portion of the study area (Fig. 1; (Agyei-Duodu et al., 2009).). Biotite granitoids intrude the volcaniclastic and pelitic rocks (Fig. 1). These granitoids are dated between 2116 – 2092 Ma (Amponsah et al., 2023; Sakyi et al., 2024). Generally, these rocks have undergone regional greenschist facies metamorphism (Agyei-Duodu et al., 2009). Structurally, the rocks of the study area foliated and folded.

2.2. Soil sampling

The study analysed a total of 720 samples. To cover the study area and capture soil variability, a grid-based sampling approach was used which covered the area considering the various usages of land (mining and agriculture). It was divided into equal cells suitable for systematic sampling with representative distribution of samples. Systematic sampling is vital for monitoring mining areas because contamination often displays complex spatial distribution from localized pollution sources, including tailings, pits and waste dumps. Composite samples were collected from the B-horizon at a depth of 20 cm to evaluate subsurface properties. The B-horizon was selected for sampling because it serves as a stable layer that effectively binds pollutants to its clay and mineral content. The chosen depth enables long-term ecological and health risk assessments since it tracks both root-zone interactions and provides standardized reference points for cross-study pollution comparisons. The analysis of the B-horizon provides better accuracy in detecting actual contamination levels since illegal mining activities usually involve the mobilization of subsurface materials. Using standardized tools eliminated the variability and contamination. Protocols to ensure samples met their potential were followed, involving careful sample processing in the field, labelling with relevant information, storage in cool conditions, air drying and sieving for laboratory analysis.

2.3. Analytical procedures

A composite sampling technique was used to collect the soil samples by taking three separate samples from each location, blending and homogenizing to average small-scale variability. The Ghana Geological Survey Authority (GGSA) analysed these samples. The samples were dried to constant weight for 72 hours at room temperature to reduce apparent moisture content and then oven-dried. Further, the samples were sieved through 2 mm mesh size followed by grinding to uniform fine particles with an agate mortar and pestle.

These dried and ground samples were subsequently compacted into pellets and analysed for elemental analysis using an Energy Dispersive X-ray Fluorescence (ED-XRF) spectrometer. The spectrometer was run 50 kV and 1 mA; each sample was analysed three times for accuracy. To measure the concentration of a variety of elements, including heavy metals (i.e. As, Ba, Co, Cr, Cu, Ni, Pb, V and Zn), the samples' X-ray spectra were recorded. Periodically, control samples were used to identify contamination or instrumental issues and to verify the repeatability and comparability of results.

The inclusion of Zn and Co in HHRA makes sense because these elements exist commonly in the environment and present potential health risks even though they are less harmful than Pb and As. Accurate monitoring along with regulatory actions become essential to protect human health since essentiality creates a complex relationship with toxicity, particularly in contaminated areas that combine mining-related soil pollution with agricultural exposure paths. A thorough assessment of PTE risks should focus on toxic and moderately toxic elements to create better guidelines for community protection strategies.

2.4. Quality assurance and quality control analysis (QA/QC)

Quality control was tightly adhered to thus ensuring the credibility of the soil sampling and analysis results was done according to best international practice. Every twenty field samples, with duplicates, were analysed for control reference materials (CRMs) to verify elemental analysis accuracy and to align with reference standards. This permitted the study to be able to identify and correct measured inconsistencies.

Recovery and repeatability were determined in about 5 % of the total field samples by duplicating approximately 36 samples. In both of the methods, original and duplicate samples were individually analysed, with an acceptable variation (1.3–9.2 %; see Fig. S1) of the elemental concentrations as suggested by Kwayisi et al. (2024). The United States Environmental Protection Agency (USEPA) guidelines for energy-dispersive X-ray fluorescence (ED-XRF) validation indicate that acceptable duplicate recovery rates fall within 80–120 % when conducting quality assurance and quality control (QA/QC) (USEPA, 2007). The coefficients of variation for accuracy and precision were maintained in these quality control measures to yield accurate results. Consistency between the original and duplicate samples indicated that the data was adequate for further scientific interpretation such as that in contaminated soils and environmental impacts.

The research methodology establishes a comprehensive framework for soil sampling that minimizes biases through mechanisms which prevent seasonal effects together with instrument constraints and sampling borders. This study incorporates certified reference materials, multiple analyses, and rigorous QA/QC steps to maintain data reliability even though XRF spectrometry currently has certain measurement challenges. The grid-based sampling provides spatial completeness of

the soil variability over a wide range of land uses while composite sampling reduces small-scale spatial variability. While minor risks of localized hotspot detection might be present they can be ignored because standardized protocols combined with careful sample handling protect the study findings' reliability.

2.5. Statistical analysis

The statistical analysis for the study was conducted using Python version 3.10.12 and Excel 2010. The correlation matrix which estimates the correlation between parameters was generated using Python. The SOM and associated component planes used for the visualization of the unique relationships between parameters were generated using Python. The PCA as well as the chord diagram for visualizing the relationships between parameters and principal components were also executed using Python. Both the deterministic and probabilistic variants of the human health risk assessment were conducted using Python as well. The summary statistic for the dataset was performed using Excel 2010.

2.6. Data preprocessing

To ensure the reliability and interpretability of the statistical and ML methods employed in the study, structured data preprocessing approaches were employed. In this study, missing values were addressed using the "Substitution using Minimum Value/2″ or "Min/2", where each missing value was replaced with the minimum recorded value divided by 2 within the respective variable. This approach minimizes data loss while maintaining the statistical integrity of the dataset. Lastly, the dataset was standardized using the standard scalar library in Python before each analysis was conducted; this prevents unstable behaviour caused by variables or values with vastly different magnitudes.

2.7. Pollution indices

To aid in the estimation of the level of pollution, the following indices were used in the study, single Pollution Index (PI) and Geochemical Index (Igeo).

2.7.1. Geochemical Index (Igeo)

Geochemical Index (Igeo) contributes to the assessment of contamination by comparing concentrations of elements in specific environments to a reference concentration. It is represented by equation (1).

$$Igeo = log_2\left(\frac{C_n}{1.5B_n}\right) \quad (1)$$

where C_n represents the metal concentration, B_n represents geochemical background values (Müller, 1981).

2.7.2. Single pollution Index (PI)

Single Pollution Index (PI) measures the pollution level of a single heavy metal in a soil sample by comparing the concentration of the metal in the sample to a reference value. It is calculated using equation (2)

$$PI = \frac{C_n}{BG} \quad (2)$$

where C_n represents concentration of the metal in the sample and BG represents the geochemical background value (Weissmannová and Pavlovský, 2017).

Table () shows the classification for both Igeo and PI.

2.8. Self-organizing maps (SOM)

Self-Organizing Map (SOM) algorithm, introduced by Kohonen (1982), was utilized in this study to cluster the relationships between variables in a dataset. SOM is a neural network model designed to create a nonlinear transformation. It maps high-dimensional input data, such as sensory or other signals, onto a lower-dimensional neural grid (Kohonen, 1997). SOMs are made up of neurons assembled onto a low-dimensional grid. The clustering process helped reveal inherent groupings within the contaminants, providing insights into their potential interrelationships and spatial distribution.

In a Self-Organizing Map (SOM), neurons are linked through a neighbourhood relationship that defines the map's topology or structure (Kirt et al, 2007). This ensures that similar entities are positioned close to each other on the grid. The training process builds the SOM nodes to represent the entire dataset, with the weights adjusted iteratively. At each iteration, a sample vector is randomly selected from the input data, and the distances between this vector and all weight vectors of the SOM are calculated using a chosen distance metric (Astel et al, 2007).

In our study, the non-hierarchical K-means clustering algorithm was employed. For the best possible set of results, the model was tuned using the Davies-Bouldin Index (BDI). At every iteration, parameters like grid dimension, learning rate, neighbourhood radius, and number of iterations were changed, ultimately, the clustering solution with the lowest Davies–Bouldin index was selected as the most effective classification (Astel et al, 2007).

2.9. Health risk assessment

The human health risk assessment conducted in the study was performed using guidelines developed by the United States Environmental Protection Agency (USEPA, 2002, 2006, 2008). A total of 3 exposure pathways were considered for the study namely, ingestion, dermal adsorption and inhalation. Two population groups were also considered for the study, adult and child.

The exposure parameters used in the human health risk assessment were selected based on established guidelines from the United States Environmental Protection Agency (USEPA) and human health risk assessment studies involving potentially toxic elements (PTEs) (Agyeman et al, 2021, USEPA, 2011, USEPA IRIS, 2024, IDNR, 2024).

Additionally, while the USEPA exposure parameters serve as a widely recognized reference point, concerns regarding its applicability to particularly children in Ghana and other parts of the world are valid. However, in the absence of comprehensive ingestion rate data from Ghana, relying on internationally accepted values ensures comparability with other health risk assessments and maintains consistency with global risk assessment practices. In regions with artisanal and small-scale mining (ASM) activities, the ingestion rates for children may indeed be higher due to increased exposure to contaminated soil and dust. To address this, uncertainty quantification through Monte Carlo simulation was employed introducing a range of exposure parameters that would capture higher ingestion rates in ASM intensives regions. Given these considerations, the exposure parameters chosen for the study remains an appropriate choice as it provides a protective estimate of exposure while aligning with international standards.

The calculation of the deterministic method was done using Python 3.10 manually implementing the calculations using the Numpy library. Visualization of the results was generated using the Matplotlib library. he probabilistic method, similar to the deterministic was also conducted using Python 3.10, the Monte Carlo simulation was manually implemented using NumPy library for random sampling of 10,000 iterations swithin defined parameter ranges namely, ingestion rate (80,120) mg/day, inhalation rate (15, 25) m^3/day, body weight (65,75) kg, exposure frequency (340, 360) days/year, exposure duration (25, 35) years, particle emission factor (PEF) (1.3e9, 1.4e9) m^3/kg, skin surface area (5500, 6000) cm^2/day, and adherence factor(0.06, 0.08) mg/cm^2 for adult. For child, ingestion rate (180, 220) mg/day, inhalation rate (6.5, 8.5) m^3/day, body weight (10, 20) kg, exposure frequency (340, 360) days/year, exposure duration (5, 7) years, particle emission factor (PEF) (1.3e9,1.4e9) m^3/kg, skin surface area (1900, 2100) cm^2/day, and

adherence factor (0.18, 0.22) mg/cm^2. Visualization of the results from the Monte Carlo simulation was also conducted using Matplotlib library.

To determine the non-carcinogenic health risk, average daily dose (ADD) for each element and each exposure pathway was calculated using equation (3). 4, 5.

$$ADD_{ingestion} = \frac{C_{soil} \times IngR \times EF \times ED}{BW \times AT} \times CF \quad (3)$$

$$ADD_{dermal} = \frac{C_{soil} \times SA \times AF_{soil} \times ABS \times EF \times ED}{BW \times AT} \times CF \quad (4)$$

$$ADD_{inhalation} = \frac{C_{soil} \times InhR \times EF \times ED}{PEF \times BW \times AT} \quad (5)$$

Where ADD represents the average daily doses for ingestion, dermal, and inhalation, C_{soil} is the concentration of the contaminant in the soil, IngR represents ingestion rate, InhR represents inhalation rate, EF represents the exposure frequency, ED, exposure duration, CF, the conversion factor, BW, average body weight, AT, average time, ABS represents, absorption factor, SA, surface area, and PEF, particle emission factor (Nikolaidis et al, 2013). The values for the exposure parameters as well as references doses and cancer slope factors for both adult and child are shown in tables 1 and 2.

3. Results and discussion

3.1. Summary statistics of the PTEs in the area

Table 3 is a summary of the results determined for the selected PTEs in the study area. A summary statistics table containing all relevant information regarding the data used in the study was generated using Microsoft Excel. All samples recorded some PTEs above their Upper Continental Crustal Averages (UCC) as shown in table 3. In decreasing order, the PTEs with the most samples above their respective UCC are; As(100 %), Ba(13 %), Cr(5.8 %), Pb(2.7 %), Co(2 %), V(2 %), Cu(0.4 %) and Zn(0.4 %). Ni reported just one (1) sample above its UCC values of 75 mg/kg. According to Chen et al. (2008) the Coefficient of Variation (CV) is generally applied to evaluate soil elemental variability and to infer their possible sources based on three levels derived from their corresponding CV values; Weak variability (natural sources) is indicated by CV < 0.1; moderate variability (natural and anthropogenic sources) is $0.1 \leq$ CV < 1; and strong variability, or extrinsic or anthropogenic sources, is denoted by CV ≥ 1. The samples reported CV values ranging between 0.40 and 0.98, signifying varying degrees of natural and anthropogenic influences on the spatial variability of the PTEs in the area. The CV values of V(0.40), Cr(0.41), Co(0.49), Cu(0.50), Ba(0.51) and Zn(0.53) showed a mixed source of geogenic and anthropogenic influence on the distribution of those PTEs. Ni(0.65), As(0.72) and Pb (0.98) showed values suggestive of a significant degree of anthropogenic influence on their variance across the study area.

As values across the area fall below the threshold (13.29 mg/kg) established by Kazapoe and Arhin (2019) in the southwest of Ghana within a similar geological setting. The reported CV along with the skewness and kurtosis values of 1.63 and 3.50, suggests that its distribution across the area is influenced by anthropogenic activities with the presence of some hotspots. The range of figures determined for As are similar to values reported in stream sediment samples collected from the Birim (35.01 mg/kg) and Subri (31.82 mg/kg) rivers from the south of Ghana by Hadzi et al. (2023). The reported values have a wider range than what was reported (1.7 – 2.4 mg/kg) from the Marlu tailings dam near Bogoso in the Western region of Ghana (Doku and Belford, 2022). They are however relatively elevated (0.5 – 1.3 mg/kg) as compared to mining communities around Kyebi in southeastern Ghana (Opoku et al., 2024). These values contrast with As values, determined in non-mining areas in the same geological settings by Obiri et al. (2016) who recorded a range between 0.8 to 1.1 mg/kg. The pattern of As distribution in mine spoils around active mines in Ghana was found by Mensah et al. (2020) to be controlled by amorphous Fe oxides contents, sulphides and As-bearing minerals. Marschner et al. (2020) agree with this, as they state that arsenic is often associated with As-bearing minerals such as scorodite and arsenopyrite. The sulphide complexes are known to be commonly related with gold mineralisation in Ghana (Kazapoe et al., 2023).

Similarly, Ba shows a value (196.1 mg/kg) which is far above the value reported by Crommentuijn et al. (2000: 4.5 mg/ kg). The current study reported values averagely (6.82 mg/kg) similar to values reported by Kazapoe and Arhin (2019). Ni exceeded the WHO limit of 35 mg/kg in only eight (8) samples. Moreover, their CV further indicates moderate anthropogenic influence in their distribution. Ni values, however, were found to be largely higher than the 0.20–0.68 mg/kg determined by Mensah et al. (2015b) in Damang-Abosso which is also a recognised

Table 1
Exposure parameters for child and adult used in the calculation of the human health risk assessment.

IngR (Adult)	100 mg/d
IngR (Child)	200 mg/d
InhR (Adult)	20 m^3/day
InhR (Child)	7.65 m^3/day
EF (Adult)	350d/y
EF (Child)	350d/y
ED (Adult)	30y
ED (Child)	6y
AT	ED*365d/y
BW (Adult)	70 kg
BW (Child)	15 kg
SA (Adult)	5800 cm2/d
SA (Child)	2000 cm2/d
AF (Adult)	0.07 mg/cm2
AF (Child)	0.2 mg/cm2
PEF	1.36 × 109 m3/kg

Source: USEPA, 1991, 2002b, 2011, 2013.

Table 2
Reference doses and cancer slope factors for each PTE used in the calculation of the human health risk assessment.

Ingestion			
As_RfD	3 x 10—4 mg/kg-day	As_CSF	1.5 mg/kg-day
Ba_RfD	0.2 mg/kg-day	Ba_CSF	–
Cr_RfD	0.003 mg/kg-day	Cr_CSF	0.27 mg/kg-day
Co_RfD	0.0003 mg/kg-day	Co_CSF	–
Cu_RfD	4.0*10–2 mg/kg-day	Cu_CSF	–
Ni_RfD	2*10–2 mg/kg-day	Ni_CSF	0.8 mg/kg-day
Pb_RfD	3.50*10–3 mg/kg-day	Pb_CSF	0.28 mg/kg-day
V_RfD	0.007 mg/kg-day	V_CSF	–
Zn_RfD	3*10–1 mg/kg-day	Zn_CSF	–
Dermal			
As_RfD	0.0003 mg/kg-day	As_CSF	1.5 mg/kg-day
Ba_RfD	0.014 mg/kg-day	Ba_CSF	–
Cr_RfD	0.0195 mg/kg-day	Cr_CSF	0.27 mg/kg-day
Co_RfD	0.0003 mg/kg-day	Co_CSF	–
Cu_RfD	0.04 mg/kg-day	Cu_CSF	–
Ni_RfD	0.0008 mg/kg-dy	Ni_CSF	0.8 mg/kg-day
Pb_RfD	0.04 mg/kg-day	Pb_CSF	0.28 mg/kg-day
V_RfD	0.00013 mg/kg-day	V_CSF	–
Zn_RfD	0.3 mg/kg-day	Zn_CSF	–
Inhalation			
As_RfD		As_CSF	15.1 mg/m3-1
Ba_RfD	0.0005 mg/m3	Ba_CSF	–
Cr_RfD	0.001 mg/m3	Cr_CSF	0.27 mg/m3-1
Co_RfD	6*10–6 mg/m3	Co_CSF	–
Cu_RfD	4.02*10–2 mg/m3	Cu_CSF	–
Ni_RfD	0.0002 mg/m3	Ni_CSF	0.8 mg/m3-1
Pb_RfD	3.52*10–3 mg/m3	Pb_CSF	0.28 mg/m3-1
V_RfD	0.0001 mg/m3	V_CSF	–
Zn_RfD	3*10–1 mg/m3	Zn_CSF	–

Source: Agyeman et al, 2021, USEPA, 2011 USEPA IRIS, 2024, IDNR, 2024.

Table 3
Summary statistics of the PTEs measured from the study area.

	Minimum	Maximum	Mean	Median	Standard Deviation	Kurtosis	Skewness	Coefficient of Variation
As	2	48	9.68	8	7.01	3.50	1.63	0.72
Ba	4	556	196.21	198	99.31	0.014	0.26	0.51
Co	4	20.8	6.82	5.6	3.34	1.28	1.30	0.49
Cr	16	253	84.09	76	34.76	0.96	0.94	0.41
Cu	4	59	12.23	11	6.12	6.54	1.75	0.50
Ni	2	78	11.59	10	7.58	8.91	1.97	0.65
Pb	5	148	7.43	5	7.31	195.75	11.33	0.98
V	8	189	74.74	73	30.24	0.17	0.49	0.40
Zn	10	187	31.30	27	16.54	14.17	2.52	0.53

mining region that has similar geology. However, these numbers are the same as those reported by (Kazapoe et al., 2022) from a similar area of southwestern Ghana (2.00–71.00 mg/kg). Similar results were seen in this study compared to Opoku et al. (2020)and Baah et al (2023), who worked in southern Ghana. Despite these findings, which also reported higher levels of Ni, they found the levels were below a contaminant threshold of 35 mg/kg established by the WHO. The majority of the samples recorded Pb concentrations between 5 and 37 mg/kg and despite Pb's relatively high maximum values (148 mg/kg), Pb concentrations in the majority of the samples were relatively low. Broadly similar findings have been reported by Baah et al. (2023) in a mining area of the Ashanti region of Ghana (35,1–49.4 mg/kg). Like Pb, which is known to be naturally occurring and bioaccumulates in soils (Ogundele et al., 2015), its relatively high CV (0.98) reflects a significant anthropogenic influence on its overall distribution. The reason Pb exists in the soil is that of gold extraction activities that took place in parts of the Ashanti region which very much corresponds with the Wassa Amenfi traditional area (Amoakwah et al., 2020). Conversely, V and Zn had average values (74.74 and 31.30 mg/kg) lower than their UCC (135 and 70 mg/kg, respectively) and CV (0.40 and 0.52) respectively, suggesting a geogenic influence on their general distribution across the study area. The PTEs displayed a decreasing trend in the order Ba > Cr > V > Zn > Cu > Ni > As > Pb > Co which closely mirrors what was reported by (Rudnick and Gao, 2003) for the upper continental crust (Ba > V > Cr > Zn > Cu > Co > Pb) except for the Cr vs V and Co vs Pb. This is suggestive of a degree of human interference.

3.2. *Correlation matrix*

The correlation matrix heatmap (Fig. 2) was generated using Python 3.10 employing a combination of Seaborn and Matplotlib libraries. The correlation matrix outlines PTEs with significant correlation, moderate correlation and a third group with very low correlation. The first group shows a strong correlation of V with Ba(0.70), Cr(0.69), Cu(0.61) and Ni (0.65). Additionally, Ni and Ba are strongly correlated with Cu(0.67) and Cu(0.65) respectively. This implies a probable common geogenic origin or similar environmental control on their distribution in the soil. These elements are frequently linked with mafic and ultramafic lithologies, which characterize most of the Birimian terrain. Ferromagnesian minerals are abundant in mafic rocks, which can weather to give rise to

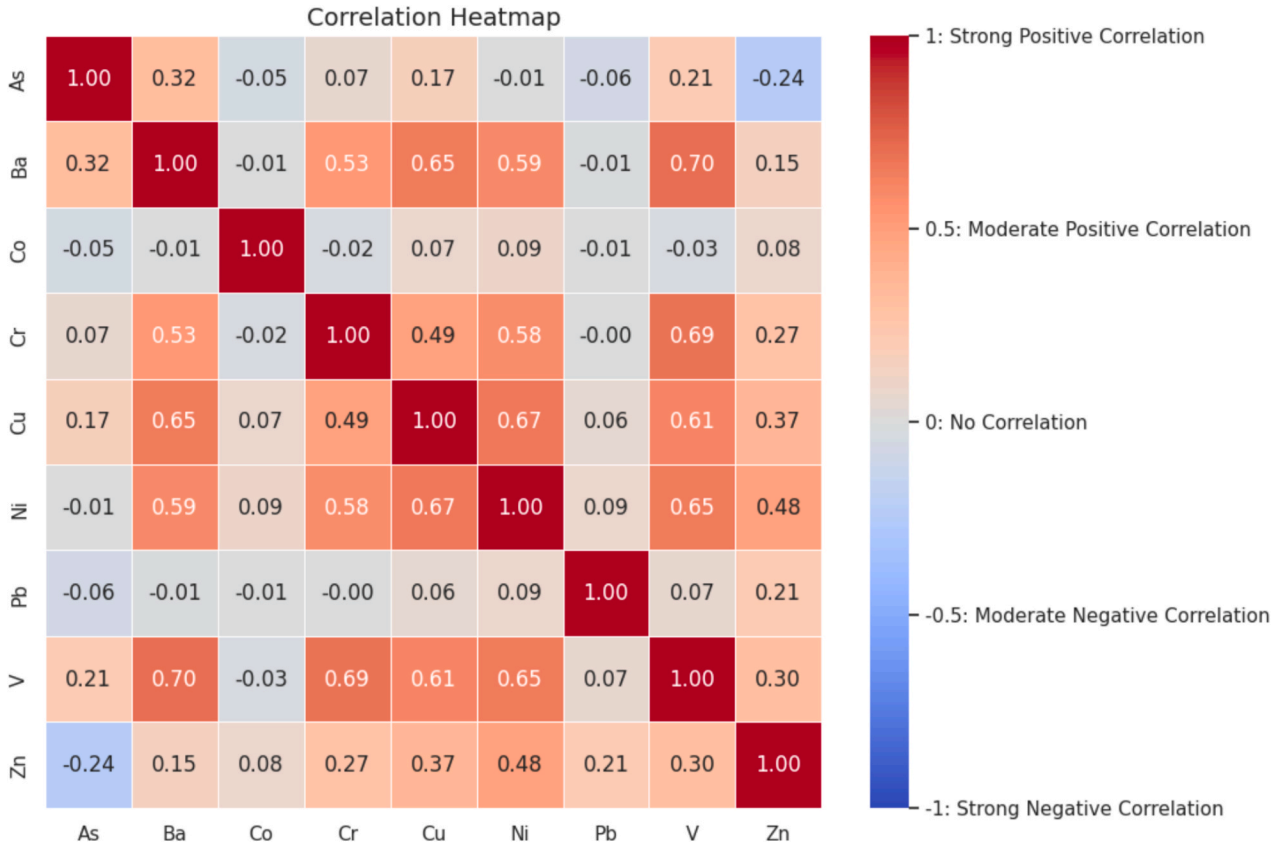

Fig. 2. Correlation heatmap of PTEs in the study area.

these metals in the soil (Taylor and McLennan, 1985).

Cr and Cu moderately correlates with Ba(0.53) and Cr(0.49) respectively. Cr is similarly associated with ultramafics and spinel group minerals. The correlation with Ba and Cu may indicate localized Cr interactions or secondary processes like partial Cr release during weathering and incorporation of Cr into clays or oxides (Oze et al., 2007). The moderate Cr and Cu relationship might reflect spatial variability in the mineral distribution or degrees of weathering and mobility of these elements in soil.

The third is comprised of As and Pb, which report low to no correlation with all the other PTEs. The absence of such association suggests that the elements in the study area are different in origin or that these elements exhibit different geochemical characteristics. For example, As is known to be associated with sulfide minerals such as arsenopyrite (e.g. arkose sandstone), and may have been introduced locally by hydrothermal activity or anthropogenically through mining (Smedley and Kinniburgh 2002a). Pb, however, is commonly bound with galena or anthropogenic activities such as mining, smelting and vehicular emissions (Alloway, 2013). Isolation of As and Pb from other PTEs reflects a lack of correlation between As and Pb with the other PTEs, suggesting that these elements could originate from unique source(s) or have limited mobility and redistribution in soil under the prevailing soil conditions.

3.3. Principal component analysis

Principal Component Analysis (PCA) in the study was conducted using Python 3.10, employing libraries such as Seaborn, Matplotlib, and Factor Analyzer. Generation of the chord diagram and scree plot also employed Python 3.10 using the Pycircilize and Matplotlib libraries respectively. Table 4 shows the results from KMO measure of sampling adequacy and Bartlett's test of sphericity. The measure of sampling adequacy was found to be 0.827 satisfying the necessary condition of $>$ 0.5. The significance value for Bartlett's test was 0.000 fulfilling the requirement of ($p < 0.001$). Table 2 and Fig. 3 show the percentage of variance explained by each component as well as the contributions made by each metal. Eigen values were used as the criteria for the selection of principal components. From Fig. 3 and Table 5, three principal components have eigen values above 1, therefore three principal components were selected namely PC1, PC2, and PC3.

Contributions on PC1 are indicated by the colour purple, contributions on PC2 are outlined as lemon green while that of PC3 is yellow on the chord diagram (Fig. 4). The thickness and direction of the connecting chords illustrate the strength and nature of the relationship between the metals and the components. PC1 explains the largest variance (41.000 %; Table 5), Ba, Cr, Cu, Ni, and V are indicated are the most prominent chords connecting to PC1. PC2 explains about 16.02 % of the variance, the notable chords connecting to PC2 are from As, and Zn. PC3 explains about 11.30 % of the variance, visible chord connections are from Co and Pb.

PC1 further corroborates the association established by the correlation matrix (Fig. 2). These elements likely indicate a mixed source involving both natural and anthropogenic influences. Mafic to ultramafic rocks rich in Cr, Ni and V are found in the Birimian terrain (Kazapoe et al., 2021; Amponsah et al., 2021). These can be derived from the weathering of parent rocks or residual deposits. Further, Cu and Ba likely originate from mining activities, especially artisanal and small-scale operations in the Wassa area resulting from ore processing and metal leaching (Hilson, 2002a). Mining activities may also introduce V. PC2 suggests a more distinct anthropogenic signature than PC1. In the Birimian terrain, sulfide minerals (e.g., arsenopyrite) in ore bodies make As a common by-product of gold extraction (Kazapoe, 2023). Zn can be introduced by materials of industrial origin or as a trace contaminant in ores (Adomako et al., 2010). The fact that Zn may have a lithological source and is clustered in PC2 also indicates an association between Zn and gold mineralisation. Zn frequently appears as a natural element in areas with mineralized zones that contain gold. Zn occurs as a sulfide mineral in sphalerite (ZnS) often associated with other sulfide minerals such as galena (PbS) and chalcopyrite ($CuFeS_2$), and serves as a secondary element in polymetallic mineral deposits (William 2013). The breakdown of sulfide minerals due to weathering alongside oxidation processes diverts Zn into soil formations. PC3 may imply localized contamination associated with anthropogenic activities. Pb contamination is often due to the improper disposal of industrial waste. Additionally, when leaded materials are used. Cobalt can be naturally present and also present from mining tools or as a metal processing by product (Gyasi et al., 2019).

The SOM employed in the study (Fig. 5) was executed using Python 3.10 using the Minisom library, the associated D-Matrix and U-Matrix component planes were also generated using Python 3.10, employing the Matplotlib library. The Davies-Bouldin Index (BDI) (Davies and Bouldin, 1979) is a metric employed in the evaluation of the quality of a clustering algorithm. It operates by assessing the compactness of clusters within themselves as well as their separation from each other. A DBI value closer to 0 suggests high clustering quality and is thus desirable. Multiple iterations of the clustering algorithm were conducted, with the iteration producing the lowest DBI score chosen (Xu, 2011). In the end, 4 clusters, a grid dimension of 15 × 15, a learning rate of 0.5, a neighbourhood radius (sigma) 6, and 100,000 iterations were identified as the best set of parameters at a DBI of 1.5053. The SOM comprises hexagons, each bearing a number. The numbers aid in the identification of the samples found within each hexagon, thereby assisting in the identification of the exact samples found within each cluster. Fig. 5 shows 4 distinct clusters with Cluster 1 (dark blue) dominating the upper left side of the SOM. This suggests that samples found within that area have similar characteristics. Cluster 2 (light blue) mainly occupies the bottom right side of the SOM, cluster 3 (teal) spans the bottom left side, and lastly, cluster 4 (light green) occupies the upper right side of the SOM. The boundaries between clusters suggest a transition between samples in terms of characteristics.

Fig. 6 shows component planes representing the respective distributions of features across the SOM grid. Darker regions (dark blue) indicate lower values while brighter regions indicate higher values. Further observation of Fig. 6 reveals localized high concentrations of some elements in specific regions. This trend is particularly strongest in As, Co, Cr, and Pb. The rest of the elements Ba, Cu, Ni, V, and Zn seem to have multiple high value regions suggesting their prominence in the region as a whole. Ba, Cr, Cu, Ni, V, and Zn seemingly display overlapping high value regions. The suggests that these elements might be correlated with each other.

Fig. 7 shows a spatial association between clusters 1 and 2. The results from the correlation matrix, PCA and SOM indicate that while As is associated with Ba, Cr, Cu, Ni V and Zn, suggesting a shared geogenic origin, anthropogenic processes partly control the distribution of As. Although As naturally occurs in the area in association with the sulphide minerals, the extractive processes of gold, which is closely associated with the sulphides, are partly responsible for its spatial distribution in the study area. Fig. 7 corroborates this assertion as known mining locations such as Kokoase, Kwekukrom, Asante Akyim and Sureso in the northwest, Merekete Camp in the South and Pensanom in the northeast of the area plot in cluster 1. Cluster 3 suggests localized contamination of Pb associated with anthropogenic activities.

The weak association between As and Pb levels, together with other pollutant elements, points toward human industrial activities as the

Table 4
Results for the KMO and Bartlett's test.

KMO and Bartlett's test		
KMO measure of sampling adequacy		0.827
Bartlett's test of sphericity	Approx. Chi-square	2478.193
	Sig	0.000

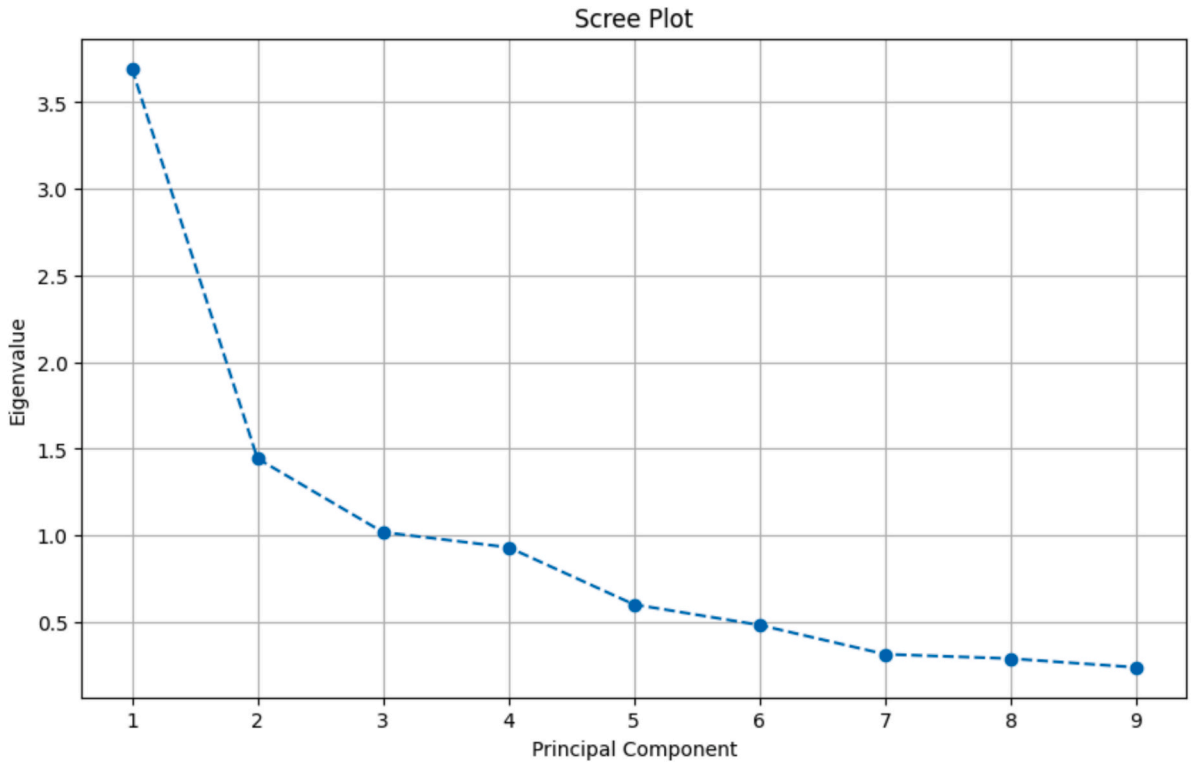

Fig. 3. Scree plot illustrating the number of principal components above the eigen value of 1.

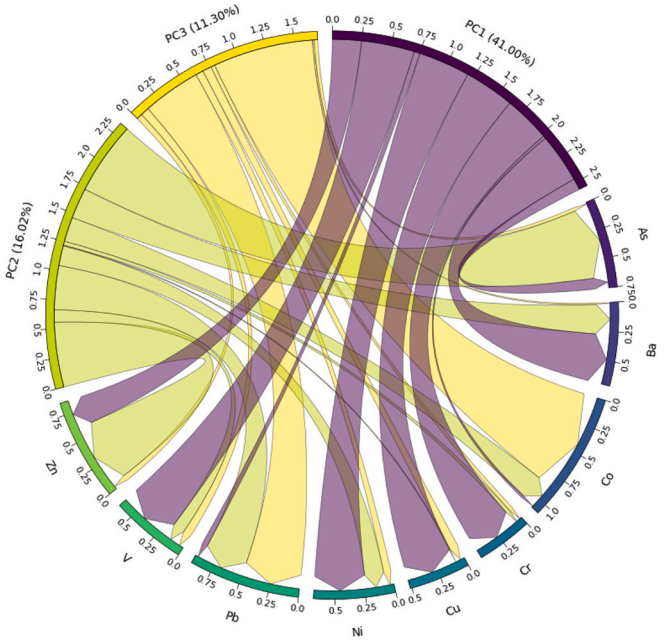

Fig. 4. Chord diagram illustrating how the variables employed in the study contribute to the 3 major principal components. The outer circular labels represent the variance explained by the 3 major principal components (PC1, PC2, PC3), as well as the elements considered in the study (As, Ba, Co, Cr, Cu, Ni, Pb, V, Zn). Loadings unto the different principal components are represented by different colours, purple for PC1, lemon green for PC2, and yellow for PC3. Thicker connections (strings) suggest stronger loadings. The principal component with the highest variance explained (PC1) lies on top followed by, PC2 and PC3 respectively. (For interpretation of the references to color in this figure legend, the reader is referred to the web version of this article.)

Table 5
Factor loadings for Components 1,2 and 3.

	PC1	PC2	PC3
Eigen values	3.695	1.444	1.018
Percentage of variance%	41.000	16.020	11.299
Cumulative percentage%	41.000	57.020	68.319

source of contamination, which stems from historical and ongoing mining operations. The geological structure of Ghana's mining areas, particularly illegal mining regions, consists of Birimian metasediments and granitoid intrusions that contain major gold deposits (Kazapoe et al., 2025). The geographical distribution of PTEs depends on mineral types found in ore deposits alongside sulfide composition and weathering conditions affecting secondary enrichment (Aryee et al., 2003). Geological conditions at artisanal mining sites powered by mercury amalgamation and cyanide leaching processes enable selective As and Pb removal, thus producing variable contamination levels across affected areas (Hilson, 2002b; Donkor et al., 2006). The combination of arsenopyrite (FeAsS) and mercury amalgamation leads to enhanced As release because of oxidation reactions, while cyanide leaching extracts Pb from minerals like galena (PbS) and cerussite ($PbCO_3$) under alkaline conditions (Smedley and Kinniburgh, 2002b).

3.4. Pollution risk indices

The results for geoaccumulation index (Igeo) and single Pollution Index (PI), are shown in Fig. 8. The results for the Igeo analysis shows that the exceedance (Igeo > 1) of the PTEs were categorised as As (58.75 %) > Cr (24.31 %) > V (0.6 %) > Cu (0.28 %) > Pb (0.28 %) > Ni (0.14 %) > Zn (0.14 %) > Ba (0 %) > Co (0 %) (Fig. 8). This depicts the spatial distribution of PTEs in the area to be uneven, with As > Cr showing significant pollution while V is slighted polluted. The mean Igeo is in the order As > Cr > V > Cu > Zn > Co > Ni > Pb > Ba. The results show that As, Cr and Pb are polluted in varying degree.

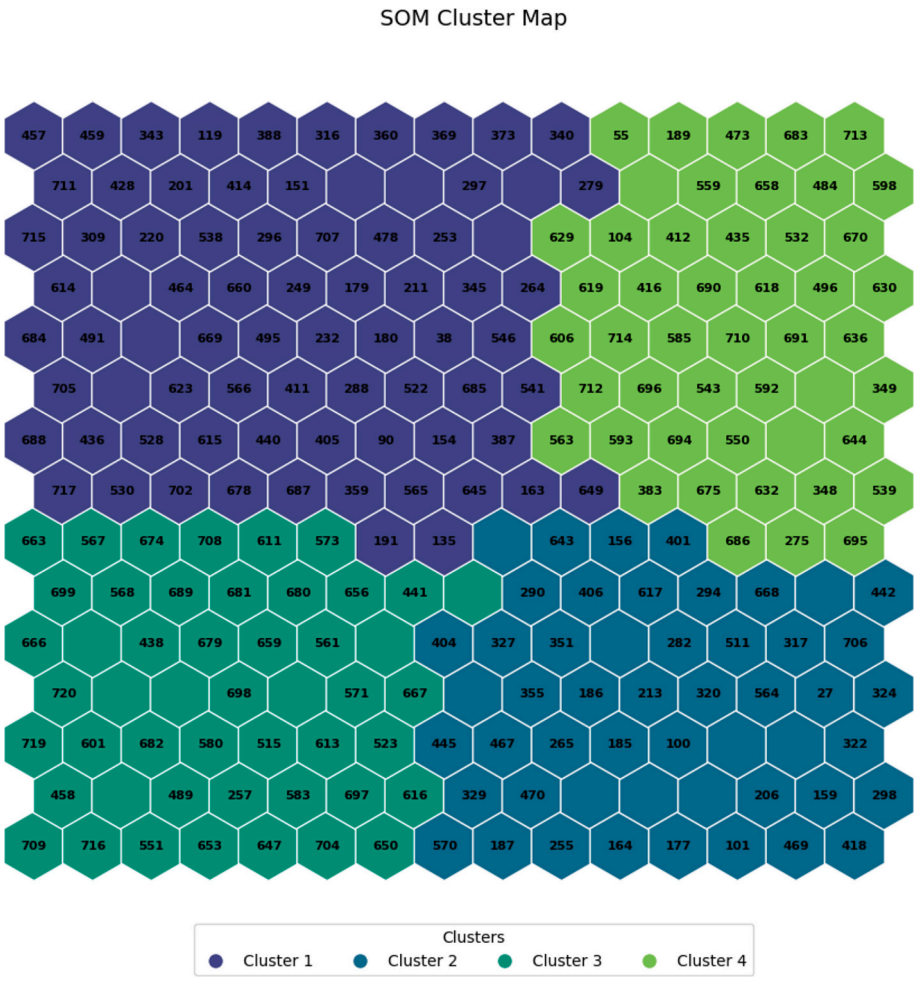

Fig. 5. Self-Organizing Map (SOM) visualizing clusters based on input data. Each hexagon represents a node, with cluster assignments color-coded from Cluster 1 (dark blue) to Cluster 4 (light blue). Sample IDs are displayed within the node, illustrating the distribution of data points across the SOM. (For interpretation of the references to color in this figure legend, the reader is referred to the web version of this article.)

The results also show that As recorded values ranging from the "unpolluted to moderately" class to "highly contaminated". The majority of the samples classed As as moderately polluted (31.11 %) and moderately to highly polluted (22.78 %). 24.17 % of the samples recorded Cr as moderately polluted. This shows the significant impact of the gold mining activities on the soil health of the area. These results differ from results obtained from a mining area in the Amansie West district of the Ashanti region where As, Pb, Cu and Ni reported Igeo values > 1 (Baah et al., 2023). Additionally, a majority of samples reported Ba(100 %) $>$ Co(99.31 %) $>$ Zn(98.89 %) $>$ Pb(97.64 %) $>$ Cu (92.36 %) and V(58.87 %) as uncontaminated.

The PI analysis showed that 15 % of the samples had low As pollution while a majority of the samples (76.67 %) cumulatively showed moderate to very strong As pollution. Similarly, 38.89 % of the samples indicated that the study area has low Cr pollution. Additionally, 33.47 % and 22.64 % of the samples are classed as moderately and strongly polluted with Cr. A majority of the samples showed that V(60.69 %) had low pollution in the area. Similar to the Igeo analysis, the PI showed that all samples had no significant pollution of Ba. Most of the samples showed that Zn(91.52 %), Ni(85.28 %), and Cu(71.52 %0 showed that pollution was absent. The Igeo and PI results further underline the growing effect of the mining-related activities on the soil quality in the area.

3.5. Deterministic human health risk assessment

The study assessed carcinogenic and non-carcinogenic health risks using both deterministic and probabilistic methods. Fig. 9 shows the distribution of values for the deterministic carcinogenic and non-carcinogenic health risk assessment for adult and child. In the non-carcinogenic risk assessment of the PTEs (As, Ba, Co, Cr, Ni, Pb, V, Zn), all values were found to be < 1 for adult, while values for child were mostly > 1, particularly beyond the 25th percentile. The adult HI values from the study area suggest that they were within the safe range since they showed values < 1 while that of children are out of the safe range of 1, indicating that PTEs within the study area pose some non-carcinogenic risk on children. For carcinogenic health risk, values for adults fell with $10^{-4} - 10^{-6}$, however, values for children mostly fell within $10^{-4} - 10^{-6}$ with a small fraction particularly within the 95th percentile exceeding the threshold. The lowest carcinogenic risk value for children (5th percentile – 0.0002) exceeds the highest carcinogenic risk value for adults (95th percentile – >0.00016) indicating higher risks for children. Though the results of the study indicate that mostly for both adults and children, the carcinogenic health risk did not exceed the threshold of $10^{-4} - 10^{-6}$ there is still some degree of carcinogenic risk in the study area. The results also show that there is a higher carcinogenic risk associated with children than adults.

Fig. 10 outlines the contributions of each PTE for the deterministic carcinogenic and non-carcinogenic health risk assessment for both adult and child. The results for non-carcinogenic health risk highlight V, Cr,

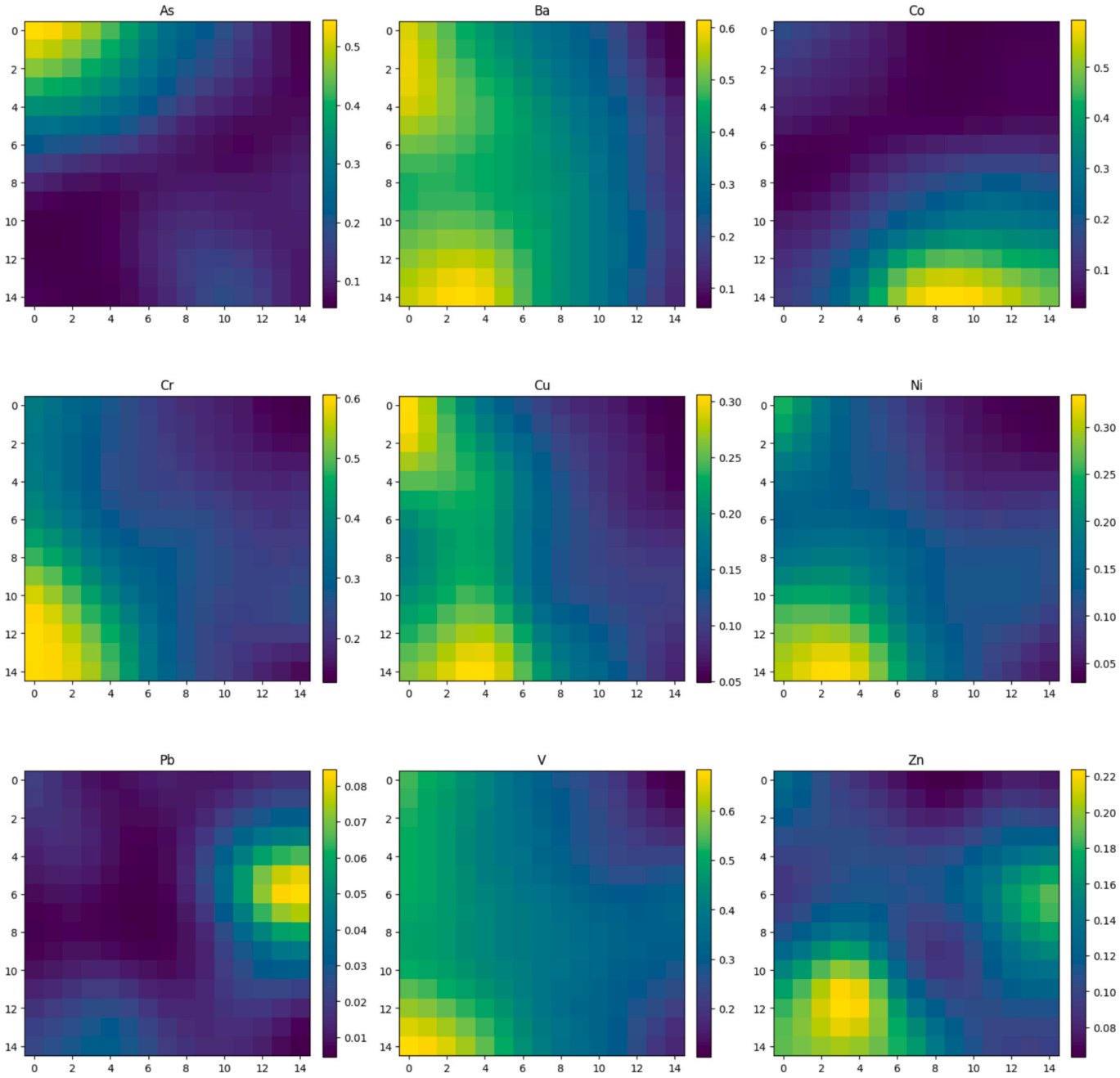

Fig. 6. Component planes for each of the elements employed in the study illustrating their distributions across the SOM.

Co, and As as the most influential PTEs for both adult and child. Contributions from As were the highest followed by Cr, Co and V. Notably, contributions for child were much higher for all metals when compared to adult. Results for carcinogenic health risk assessment show less contributions from the PTEs with just Pb, Ni, Cr, and As making contributions. Cr made the highest contributions for carcinogenic followed by As, Ni, and Pb, contributions for child were higher than adult for carcinogenic as well.

Fig. 10 shows the pathway contributions for both carcinogenic and non-carcinogenic health risk assessment. The results reveal that ingestion pathway overwhelmingly contributed to both carcinogenic and non-carcinogenic health risks. More so in non-carcinogenic than carcinogenic, dermal pathway contributed quite little to particularly V. Inhalation pathway made no contribution. Mirroring results from Fig. 10, results from Fig. 11 show ingestion pathway contributed most to As, Cr, Co, and V respectively for non-carcinogenic while for carcinogenic, ingestion pathway contributed most to Cr, As, Ni, and Pb respectively. The small contribution from dermal pathway was towards V. The results of this study are similar to the findings of Ma et al. (2023) for soil samples from the Lushui City and that of Cobbina et al. (2013) for northern Ghana where oral ingestion was the major contributing factor to non-carcinogenic risk in both adults and children. Again, a study by Penteado et al. (2021) also suggested three exposure routes which is in an order of oral ingestion > dermal > inhalation by on results from a survey of urban park soils on health risk assessment. The HI values for children are way higher than for adults. This suggests that children are more prone to PTE pollution than adults within the study area, this conforms to the study of Wu et al. (2018) and Hu et al. (2020). The reason why children are more prone can be linked to what was reported by Chen et al. (2022) that “children tend to suck their fingers and high respiratory rate”. Study by Huang et al. (2022) suggest that children are at risk than adults because children are more likely to be exposed to

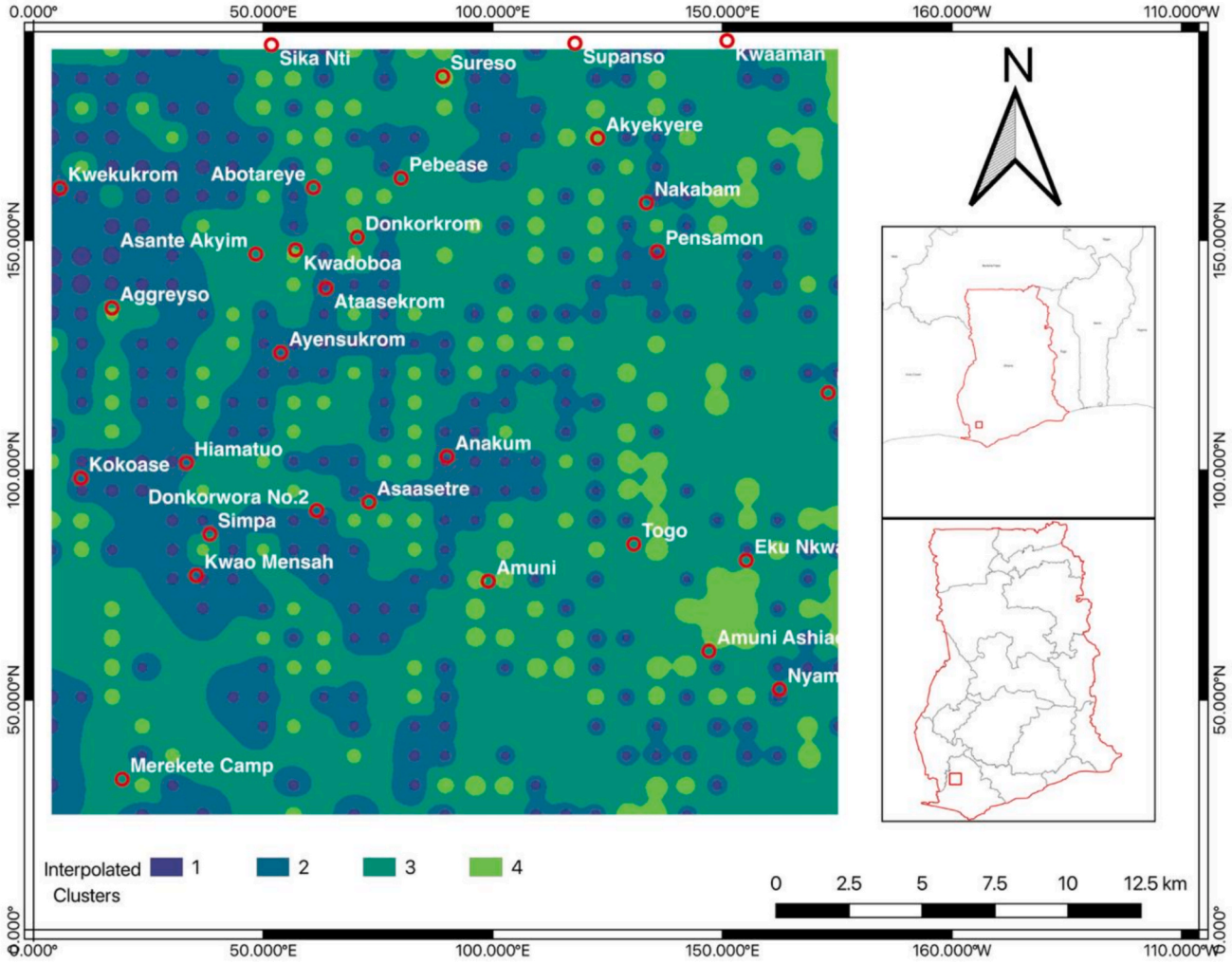

Fig. 7. Spatial representation of SOM U Matrix across the study area.

environmental pollutants. Again children (1 to 6) years tend to exhibit pica behaviour which tends to increase their intake of PTE in soils (Ghanavati et al., 2019). The study reveals that Cr is the main carcinogenic causing PTE within the study area and have higher effect on children than in adults. The results also indicate the need for interventions to help reduce the levels of PTEs that pose carcinogenic risk in children (Akakuru et al., 2023).

3.6. Probabilistic human health risk assessment

To address some of the challenges associated with deterministic health risk assessments, a probabilistic human health risk assessment was also employed. Results from Fig. 12 show that all non-carcinogenic values for adult are < 1, while that for child are mostly > 1 the exception being values from the 25th percentile below. For carcinogenic health risk assessment, all values for adult fall within the threshold of $10^{-4} - 10^{-6}$, values for child mostly meet the threshold as well the exception being mostly the 95th percentile for child. Notably, values for child are higher than that of adult.

Comparable to the deterministic method, V, Cr, Co, and As contributed most to non-carcinogenic health risk assessment. Higher values were observed for child when compared to adult as well. Fig. 13 however shows a slight deviation from the results from the deterministic method. For the probabilistic method, Cr was the most influential metal, followed by As, Co, then V. This was not the case for carcinogenic health risk assessment, which mirrored results from the deterministic method with Cr contributing highest followed by As, Ni, and Pb. This deviation could be attributed to the fact that the deterministic method employs a single estimate for each parameter, in contrast to the probabilistic which incorporates variability across range of values. This ensures that key exposure parameters vary across iterations and thus could result in higher percentiles compared to other metals. This makes the probabilistic method better account for uncertainty through the simulation of different scenarios making its results more realistic compared to the deterministic method where results serve as a useful baseline.

Besides the small deviation observed between Cr and As for non-carcinogenic health risk assessment in Fig. 13, the results for pathway contributions are also similar to that of the deterministic method. Ingestion pathway dominates the pathway contributions for all the metals. The small contribution from V observed in Fig. 11 is also observed in the probabilistic method in Fig. 14. Pathway contributions for carcinogenic remains the same as the deterministic method.

These results call for the establishment of a governance system that includes public supervision, media reporting, and public opinions which can strengthen policy effectiveness. This diverse approach has been shown to help achieve health risk control objectives by ensuring transparency and accountability in environmental management (Sun et al., 2024; Sun et al., 2025).

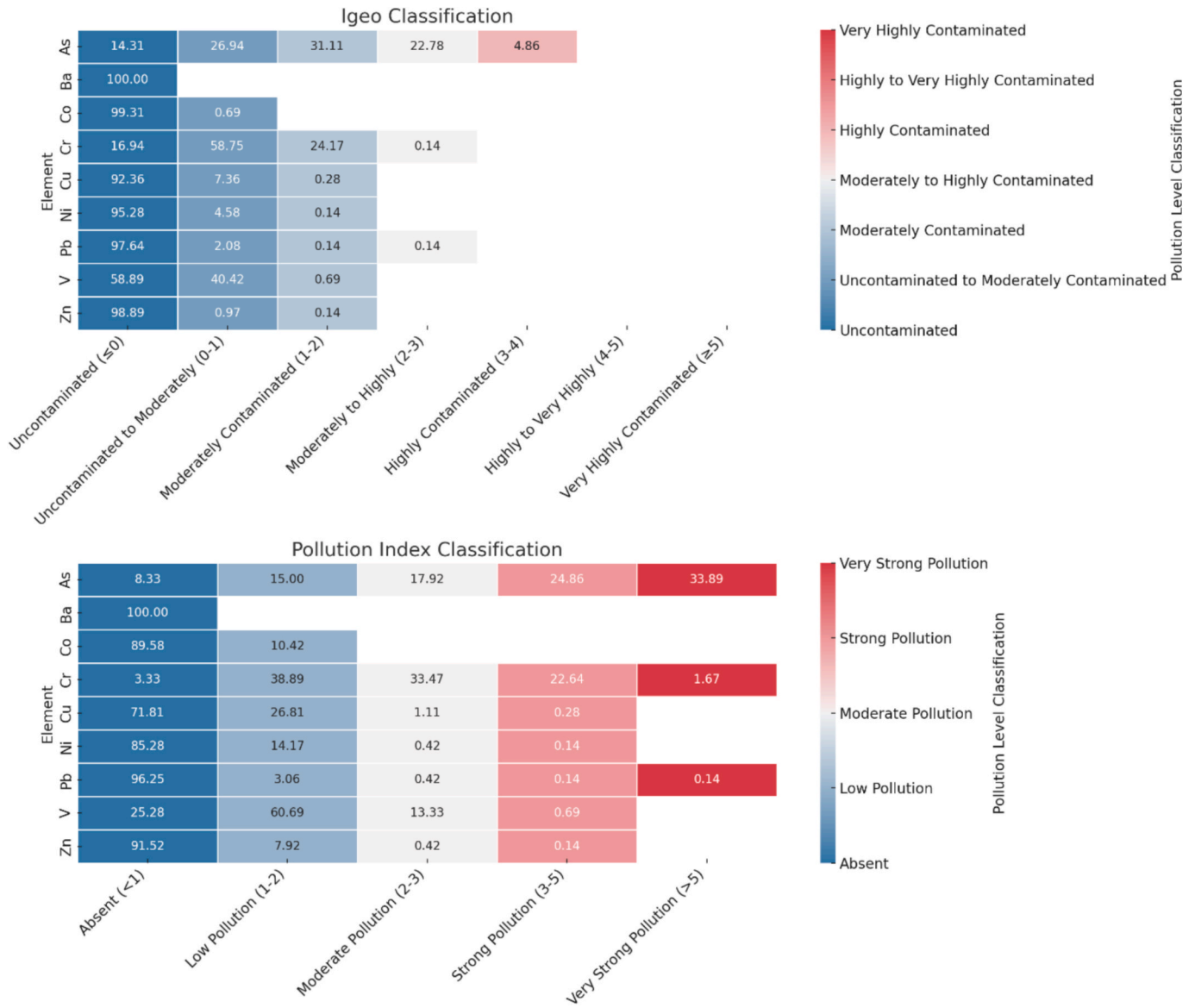

Fig. 8. Classification of heavy metal contamination levels based on the Geo-accumulation Index (Igeo) and Pollution Index, illustrating the varying degrees of contamination and pollution intensity for different elements.

4. Conclusion

This study provides a comprehensive assessment of soil contamination by Potentially Toxic Elements (PTEs) in the Wassa Amenfi area of Southwestern Ghana, an area significantly impacted by mining activities. The results indicate that arsenic (As), Cr, and lead (Pb) are the most critical pollutants, with As being the most prevalent, found in concentrations above its geochemical background across all samples. The study reveals that the presence of these PTEs arises from a combination of geogenic sources, such as the weathering of mineral-rich rocks, and anthropogenic activities, particularly related to gold mining. This dual origin highlights the complex interplay between natural and human-induced factors in environmental contamination. The findings also demonstrate that while the hazard index (HI) values for adults remain within acceptable safety limits, those for children exceed the threshold of 1, signifying a higher susceptibility to non-carcinogenic health risks in younger populations. Similarly, probabilistic assessments of carcinogenic risks show elevated values for both adults and children, with children again being more vulnerable. The ingestion pathway is identified as the predominant route of exposure, underscoring the critical need to address soil contamination as a key environmental and public health challenge in the region. Beyond the health implications, the spatial analysis of PTE distribution underscores the uneven nature of contamination, with certain hotspots exhibiting significantly higher levels of pollution. The study highlights the importance of integrating geostatistical tools and advanced risk assessment methodologies, such as Monte Carlo simulations, to generate precise and actionable insights for environmental management. This research underscores the urgent need for targeted interventions to mitigate the adverse effects of mining activities on both the environment and human health. Addressing these challenges will require a multi-pronged approach, involving stricter regulatory enforcement, community engagement, and the adoption of innovative soil remediation strategies. Such efforts are essential to safeguarding the health of vulnerable populations and ensuring sustainable development in mining-affected communities. Based on these findings it is recommended that there is the need to:

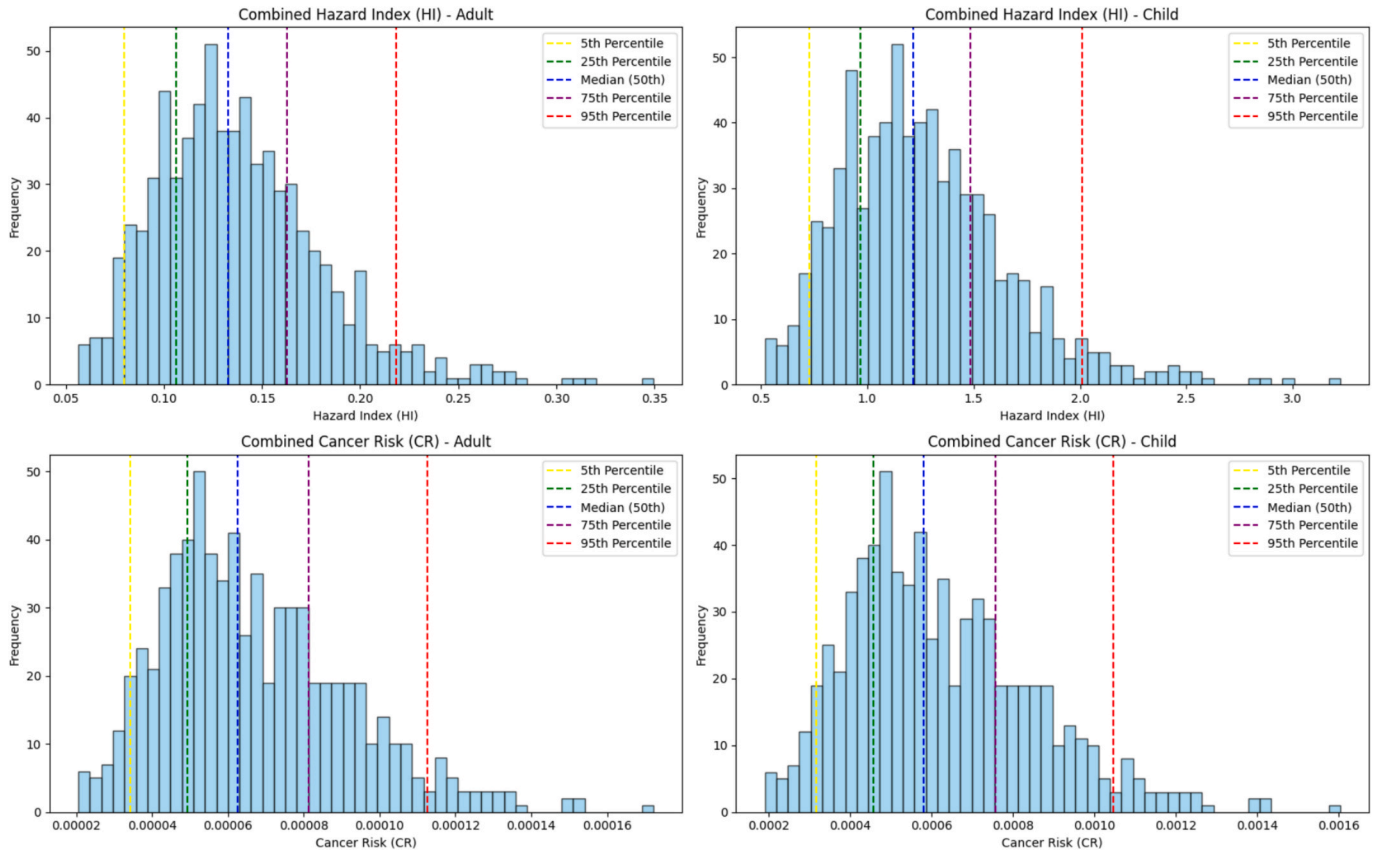

Fig. 9. Deterministic distributions of Combined Hazard Index (HI) and Combined Cancer Risk (CR) for adults and children.

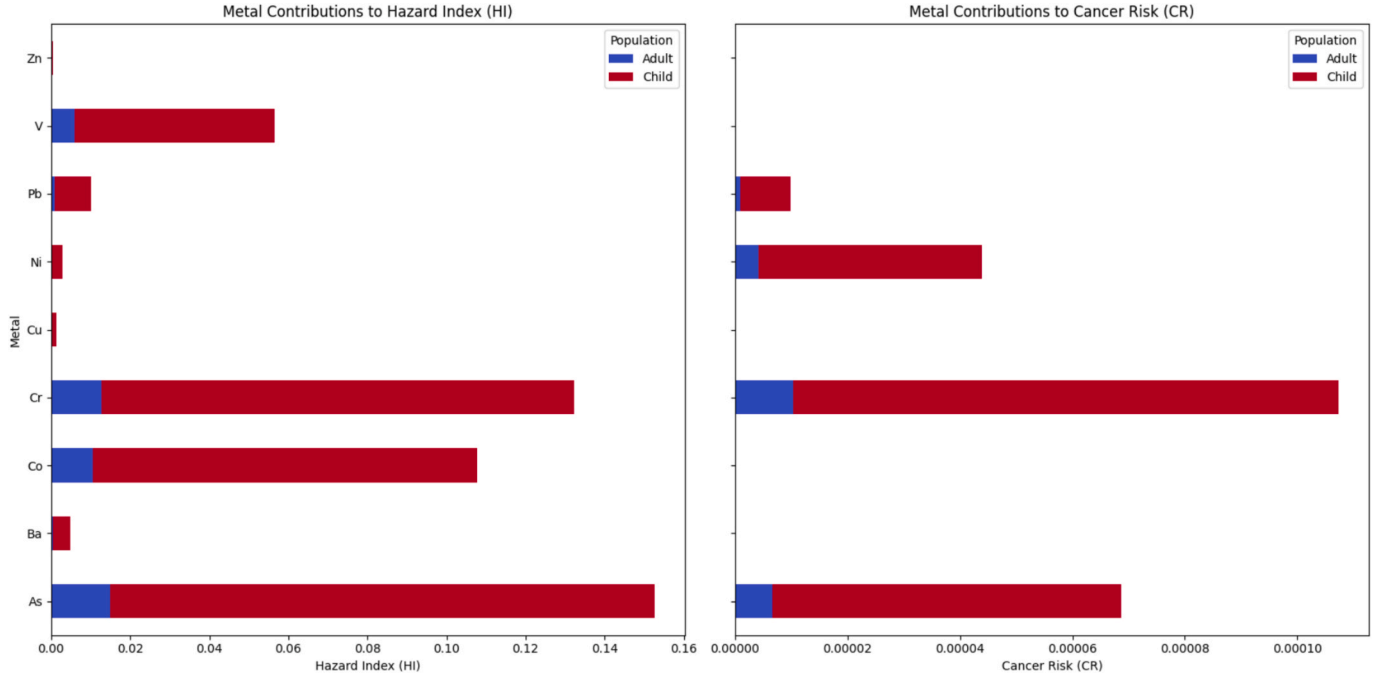

Fig. 10. Bar plots illustrating metal contributions for the deterministic method to (left) Hazard Index (HI) and (right) Cancer Risk (CR) for adults and children.

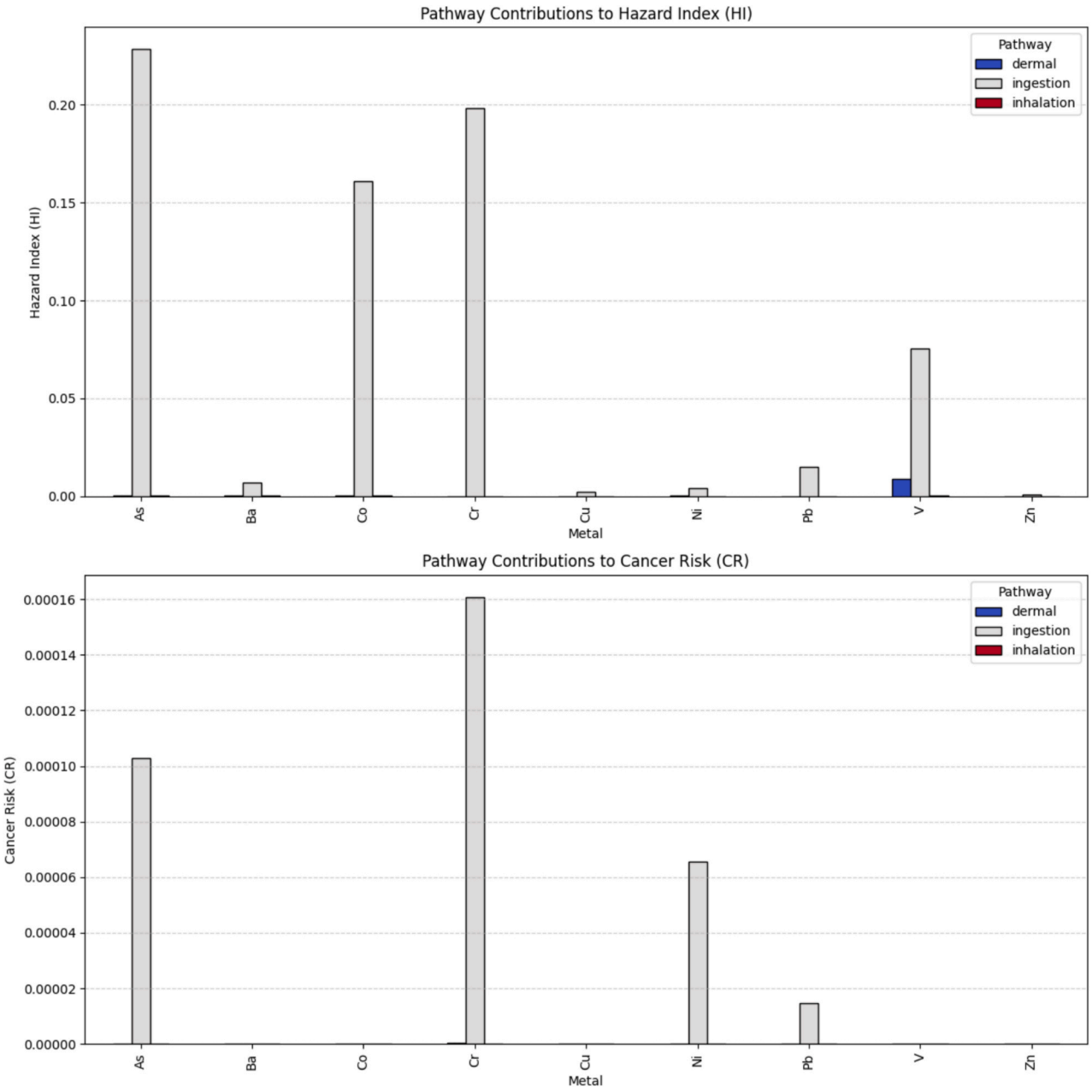

Fig. 11. Pathway Contributions to Hazard Index (HI) and Cancer Risk (CR) for Various Metals for the deterministic method: The upper chart illustrates the contributions of dermal, ingestion, and inhalation pathways to the Hazard Index (HI) for different metals. The lower chart presents the contributions of the same pathways to the Cancer Risk (CR).

- Environmental monitoring units should be decentralized while blockchain-based gold tracking should be implemented with progressive fine systems and environmental insurance and polluter-pays principles to maintain mining company accountability.
- The existing environmental regulations must be updated to establish clear limits for Pb waste disposal practices. Mining organizations must implement best practices in hazardous waste management to treat Pb-containing waste properly before disposal because this minimizes contamination risks.
- Educate community members in PTE risk management in educational institutions while establishing community-run monitoring networks and launching awareness projects to lower exposure incidents.
- A program of yearly biomonitoring should be established to study heavy metals in addition to deploying mobile health services in mining communities and building regional toxicology centers for complex medical treatments.
- The implementation of mercury-free methods such as phytomining, bioleaching and gravity separation should be supported along with providing tax benefits and training small-scale miners about eco-friendly extraction techniques for gold.
- The implementation of nano-adsorbent filtration for water sources combined with bioremediation techniques using microbes for soil detoxification and constructed engineered wetlands for heavy metal water contamination should be deployed.
- A combination of agroforestry land restoration and small-scale eco-mining cooperatives and training in organic farming, aquaculture and eco-tourism will decrease illegal mining dependency.

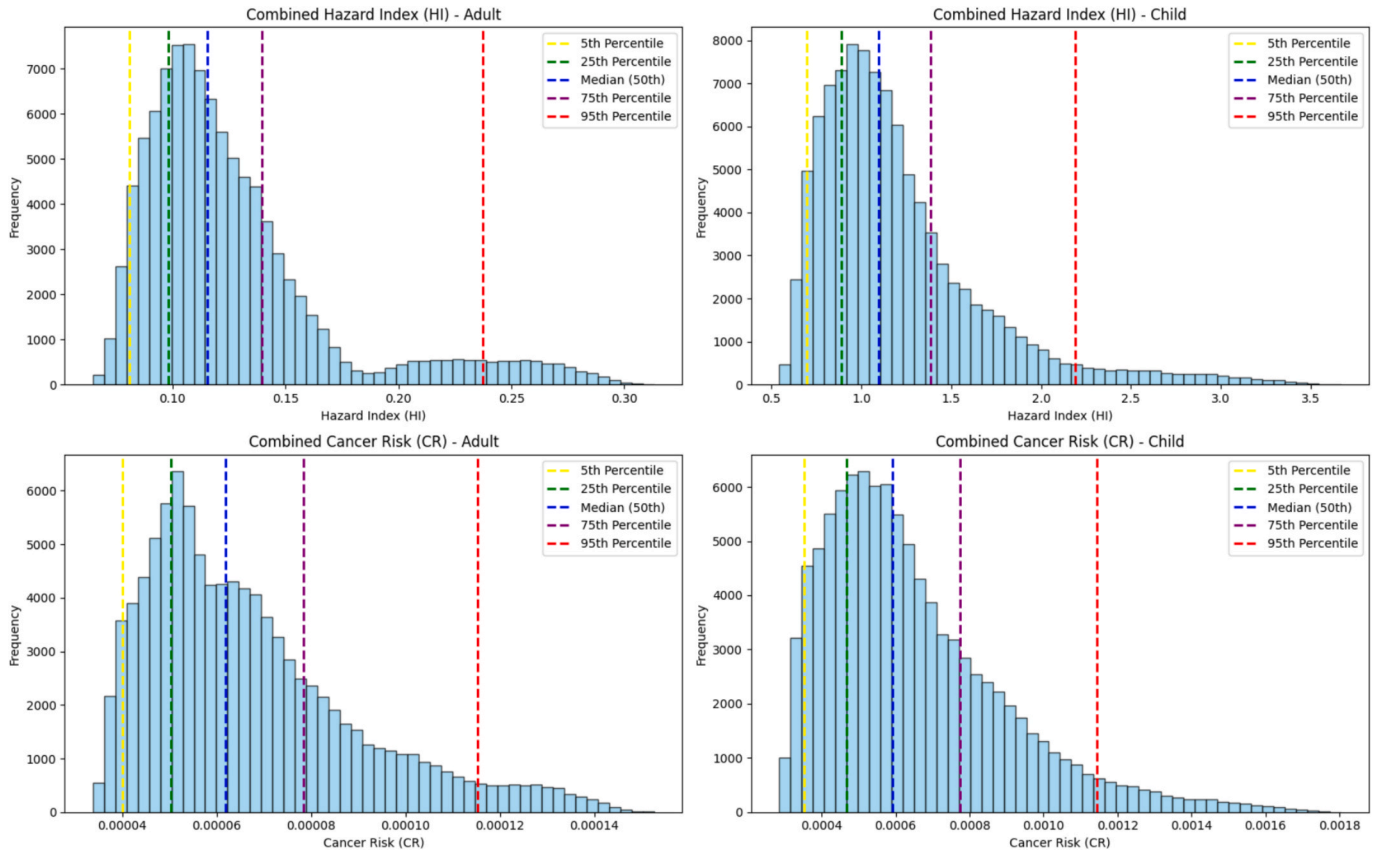

Fig. 12. Probabilistic distributions of Combined Hazard Index (HI) and Combined Cancer Risk (CR) for adults and children.

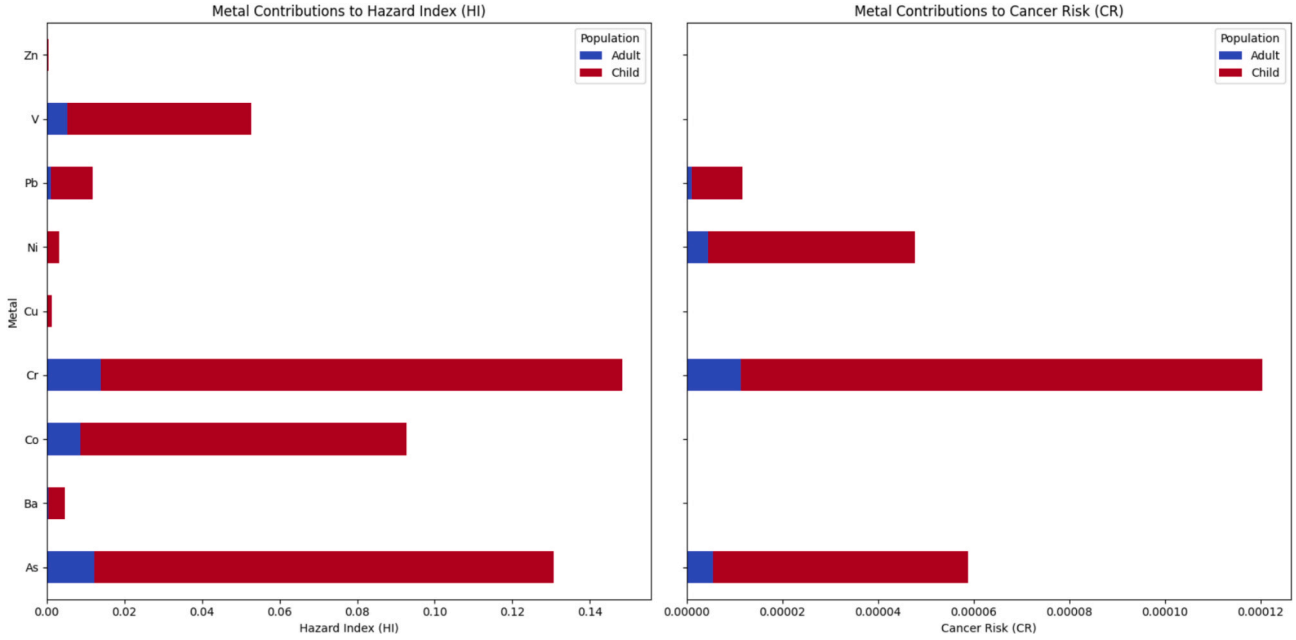

Fig. 13. Bar plots illustrating metal contributions for the probabilistic method to (left) Hazard Index (HI) and (right) Cancer Risk (CR) for adults and children.

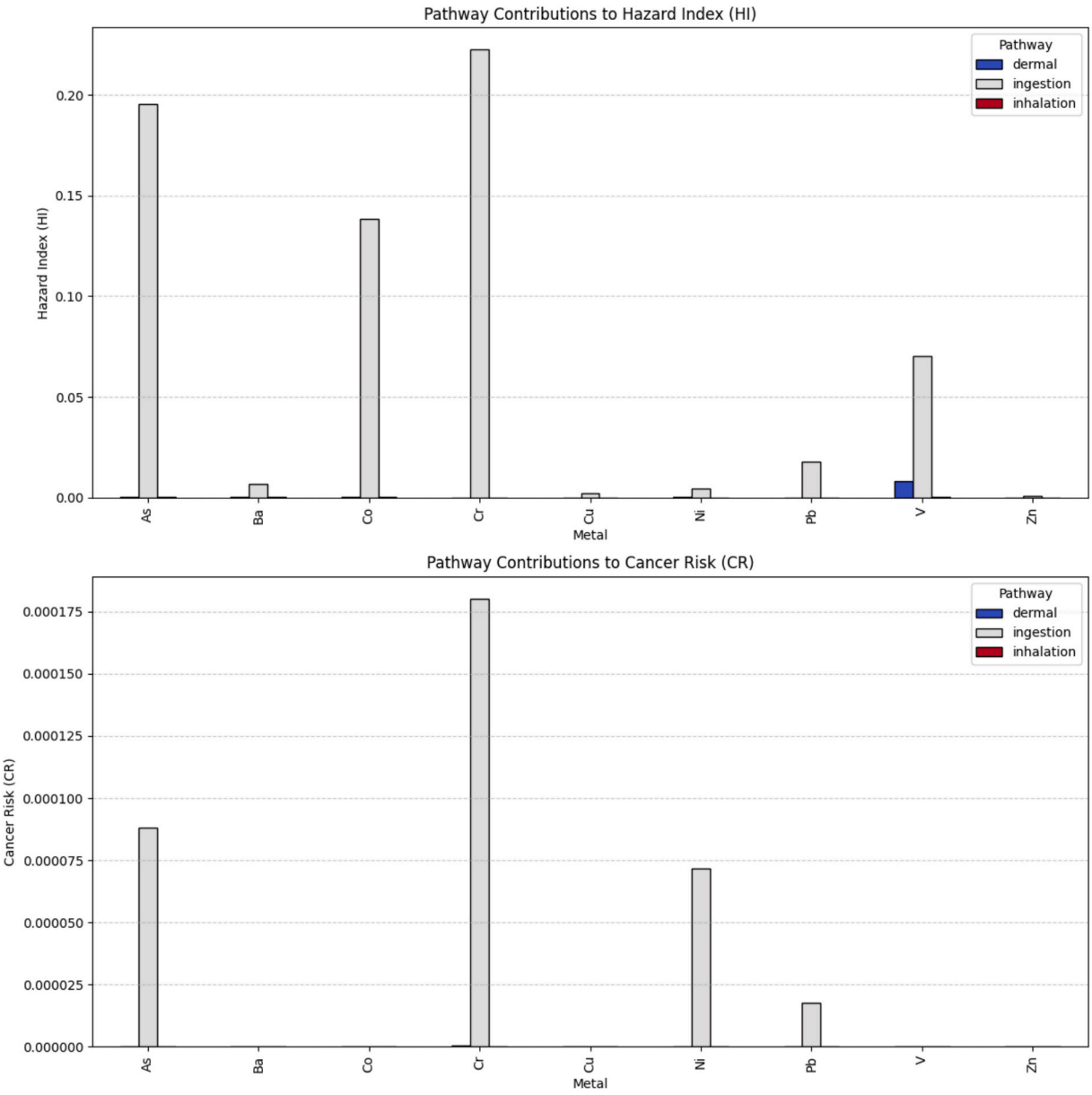

Fig. 14. Pathway Contributions to Hazard Index (HI) and Cancer Risk (CR) for Various Metals for the probabilistic method: The upper chart illustrates the contributions of dermal, ingestion, and inhalation pathways to the Hazard Index (HI) for different metals. The lower chart presents the contributions of the same pathways to the Cancer Risk (CR).

CRediT authorship contribution statement

Raymond Webrah Kazapoe: Writing – review & editing, Writing – original draft, Visualization, Validation, Supervision, Data curation, Conceptualization. **Daniel Kwayisi:** Writing – review & editing, Writing – original draft, Visualization, Validation, Supervision, Investigation, Data curation, Conceptualization. **Seidu Alidu:** Writing – review & editing, Writing – original draft, Investigation, Formal analysis. **Samuel Dzidefo Sagoe:** Writing – review & editing, Writing – original draft, Visualization, Validation, Methodology. **Ebenezer Ebo Yahans Amuah:** Writing – review & editing, Writing – original draft, Validation, Software, Methodology, Data curation. **Obed Fiifi Fynn:** Writing – review & editing, Writing – original draft, Visualization, Validation, Software, Methodology, Data curation. **Pearl Ama Ndo:** Writing – review & editing, Validation, Software, Methodology. **Portia Annabelle Opoku:** Writing – review & editing, Validation, Methodology, Data curation. **Bawa Naziru:** Writing – review & editing, Visualization, Validation, Methodology.

Funding

This research did not receive any grant from any funding agency, commercial or profit sectors.

Declaration of competing interest

The authors declare that they have no known competing financial interests or personal relationships that could have appeared to influence the work reported in this paper.

Appendix A. Supplementary data

Supplementary data to this article can be found online at https://doi.org/10.1016/j.ecolind.2025.113376.

Data availability

Data will be made available on request.

References

Adomako, D., Ayoko, G.A., Goonetilleke, A., 2010. Assessment of contamination risk of arsenic and other trace elements in groundwater and surface water in the vicinity of gold mining areas in Ghana. Environ. Monit. Assess. 165 (1–4), 561–579. https://doi.org/10.1007/s10661-009-0977-y.

Afriyie, R.Z., Arthur, E.K., Gikunoo, E., Baah, D.S., Dziafa, E., 2023. Potential health risk of heavy metals in some selected vegetable crops at an artisanal gold mining site: a case study at Moseaso in the Wassa Amenfi West District of Ghana. Journal of Trace Elements and Minerals 4 (June), 100075. https://doi.org/10.1016/j.jtemin.2023.100075.

Agyeman, P.C., John, K., Kebonye, N.M., Borůvka, L., Vašát, R., Drábek, O., Němeček, K., 2021. Human health risk exposure and ecological risk assessment of potentially toxic element pollution in agricultural soils in the district of Frydek Mistek, Czech Republic: a sample location approach. Environ. Sci. Eur. 33, 1–25.

Alloway, B.J., 2013. Heavy Metals in Soils: Trace Metals and Metalloids in Soils and their Bioavailability, (3rd ed.). Springer.

Amponsah, P.O., Kwayisi, D., Awunyo, E.K., Sapah, M.S., Sakyi, P.A., Su, B.X., Lu, Y., Nude, P.M., 2023. New evidence for crustal reworking and juvenile arc-magmatism during the Palaeoproterozoic Eburnean events in the Suhum Basin, South-east Ghana. Geological Journal 58 (10), 3734–3755.

Amponsah, P.O., Yakubo, B.B., Enu-Kwesi, F., 2021. Geochemistry and mineralogy of the Birimian rocks of Ghana: implications for tectonic settings and gold mineralization. J. Afr. Earth Sc. 182, 104292. https://doi.org/10.1016/j.jafrearsci.2021.104292.

Amuah, E.E.Y., Fei-Baffoe, B., Sackey, L.N.A., Douti, N.B., Kazapoe, R.W., 2022. Understanding the distribution, source-pattern and geochemical controls of soils in an artisanal mine site during a ban on illegal mining activities: Is a ban an absolute solution? Soil Secur. 9, 100078.

Aryee, B.N.A., Ntibery, B.K., Atorkui, E., 2003. Trends in the small-scale mining of precious minerals in Ghana: a perspective on its environmental impact. J. Clean. Prod. 11 (2), 131–140.

Asare, R., Markussen, B., Asare, R.A., Anim-Kwapong, G., Ræbild, A., 2019. On-farm cocoa yields increase with canopy cover of shade trees in two agro-ecological zones in Ghana. Clim. Dev. 11 (5), 435–445. https://doi.org/10.1080/17565529.2018.1442805.

Baah, D.S., Gikunoo, E., Arthur, E.K., Agyemang, F.O., Foli, G., Koomson, B., Opoku, P., 2023. Anthropogenic Sources and Risk Assessment of Heavy Metals in Mine Soils: A Case Study of Bontesso in Amansie West District of Ghana. Journal of Chemistry (1), 6760154.

Banchirigah, S.M., 2008. Challenges with eradicating illegal mining in Ghana: a perspective from the grassroots. Resour. Policy 33 (1), 29–38.

Boakye Dankwah, D., Enu-Kwesi, F., Koomson, F., Ntiri, R.O., Asmah, E.E., 2024. Interface between artisanal and small-scale mining and cocoa farming in the Wassa Amenfi East and West Districts of Ghana. The Extractive Industries and Society 17 (January), 101418. https://doi.org/10.1016/j.exis.2024.101418.

Chen, L., Zhou, M., Wang, J., Zhang, Z., Duan, C., Wang, X., Zhao, S., Bai, X., Li, Z., Li, Z., Fang, L., 2022. A global meta-analysis of heavy metal (loid) s pollution in soils near copper mines: Evaluation of pollution level and probabilistic health risks. Science of the Total Environment, 835, p.155441.

Cobbina, S.J., Nkuah, D., Tom-Dery, D., Obiri, S., 2013. Non-cancer risk assessment from exposure to mercury (Hg), cadmium (Cd), arsenic (As), copper (Cu) and lead (Pb) in boreholes and surface water in Tinga, in the Bole-Bamboi District, Ghana. Journal of Toxicology and Environmental Health Sciences 5 (2), 29–36. https://doi.org/10.5897/JTEHS12.0253.

Crommentuijn, T., Sijm, D., De Bruijn, J., Van den Hoop, M.A.G.T., Van Leeuwen, K., Van de Plassche, E., 2000. Maximum permissible and negligible concentrations for metals and metalloids in the Netherlands, taking into account background concentrations. J. Environ. Manage. 60 (2), 121–143.

Davies, D.L., Bouldin, D.W., 1979. A cluster separation measure. IEEE Trans. Pattern Anal. Mach. Intell. 2, 224–227.

Dong, Z., Liu, Y., Duan, L., Bekele, D., Naidu, R., 2015. Uncertainties in human health risk assessment of environmental contaminants: a review and perspective. Environment international 85, 120–132.

Donkor, A.K., Bonzongo, J.C., Nartey, V.K., Adotey, D.K., 2006. Mercury in different environmental compartments of the Pra River Basin. Ghana. Science of the Total Environment 368 (1), 164–176.

Enu-Kwesi, F., Dankwah, D.B., Ntiri, R.O., Koomson, F., Asmah, E.E., 2023. Spillover 3 Wassa Amenfi East and West Districts Ghana. African Journal of Applied Research 9 (2), 255–270. https://doi.org/10.26437/ajar.v9i2.572.

Gbedzi, D.D., Ofosu, E.A., Mortey, E.M., Obiri-Yeboah, A., Nyantakyi, E.K., Siabi, E.K., Abdallah, F., Domfeh, M.K., Amankwah-Minkah, A., 2022. Impact of mining on land use land cover change and water quality in the Asutifi North District of Ghana West Africa. Environmental Challenges 6, 100441.

Ghanavati, N., Nazarpour, A., De Vivo, B., 2019. Ecological and human health risk assessment of toxic metals in street dusts and surface soils in Ahvaz Iran. Environmental Geochemistry and Health 41 (2), 875–891.

Gyasi, R.M., Adjei, P.-O.-W., Boakye, E.A., 2019. Heavy metal contamination in mining and agriculture soils of a gold mining town in Ghana. Environ. Earth Sci. 78 (2), 37. https://doi.org/10.1007/s12665-019-8052-8.

Gyimah, N., 2019. Impact of Galamsey Operations on Agricultural Land and Livelihood of Farmers: A Case Study of Affiena Community in Wassa Amenfi West District of Western Region, Ghana. SSRN Electronic Journal. https://doi.org/10.2139/ssrn.3421765.

Hadzi, G.Y., Essumang, D.K., Ayoko, G.A., 2023. Assessment of contamination and potential ecological risks of heavy metals in riverine sediments from gold mining and pristine areas in Ghana. Journal of Trace Elements and Minerals 7 (2024), 100109. https://doi.org/10.1016/j.jtemin.2023.100109.

Hilson, G., 2002a. Small-scale mining and its socio-economic impact in developing countries. Nat. Res. Forum 26 (1), 3–13. https://doi.org/10.1111/j.1477-8947.2002.tb00199.x.

Hilson, G., 2002b. The environmental impact of small-scale gold mining in Ghana: Identifying problems and possible solutions. Geogr. J. 168 (1), 57–72.

Hou, D., O'Connor, D., Nathanail, P., Tian, L., Ma, Y., 2017. Integrated GIS and multivariate statistical analysis for regional scale assessment of heavy metal soil contamination: A critical review. Environmental Pollution 231, 1188–1200.

Hu, B., Shao, S., Ni, H., Fu, Z., Hu, L., Zhou, Y., Min, X., She, S., Chen, S., Huang, M., Zhou, L., 2020. Current status, spatial features, health risks, and potential driving factors of soil heavy metal pollution in China at province level. Environ. Pollut. 266, 114961.

Huang, C.C., Cai, L.M., Xu, Y.H., Jie, L., Chen, L.G., Hu, G.C., Mei, J.X., 2022. A comprehensive exploration on the health risk quantification assessment of soil potentially toxic elements from different sources around large-scale smelting area. Environ. Monit. Assess. 194 (3), 206.

Kazapoe, R.W., Amuah, E.E.Y., Dankwa, P., 2022. Sources and pollution assessment of trace elements in soils of some selected mining areas of southwestern Ghana. Environ. Technol. Innov. 26 (2022), 102329. https://doi.org/10.1016/j.eti.2022.102329.

Kazapoe, R.W., 2023. A review of the characteristics and geological settings of orogenic gold deposits of the Boule Mossi Domain: implication for gold exploration. Geology, Ecology, and Landscapes 1–16.

Kazapoe, R.W., Amuah, E.E.Y., Abdiwali, S.A., Dankwa, P., Nang, D.B., Kazapoe, J.P., Kpiebaya, P., 2023. Relationship between small-scale gold mining activities and water use in Ghana: a review of policy documents aimed at protecting water bodies in mining Communities. Environ. Challenges 12, 100727.

Kazapoe, R.W., Amuah, E.E.Y., Dankwa, P., Ibrahim, K., Mville, B.N., Abubakari, S., Bawa, N., 2021. Compositional and source patterns of potentially toxic elements (PTEs) in soils in southwestern Ghana using robust compositional contamination index (RCCI) and k-means cluster analysis. Environmental Challenges 5, 100248.

Kazapoe, R., Arhin, E., 2019. Determination of local background and baseline values of elements within the soils of the Birimian Terrain of the Wassa Area of Southwest Ghana. Geology, Ecology Landsc. 5 (3), 199–208.

Kazapoe, R.W., Kwayisi, D., Alidu, S., Sagoe, S.D., Umaru, A.O., Amuah, E.E.Y., Addai, M.O., Fynn, O.F., 2025. Advanced Analysis of Soil Pollution in Northeastern Ghana Using Variational Autoencoders (VAE) and Positive Matrix Factorization (PMF). *Environmental and Sustainability Indicators*, p. 100627.

Kazapoe, R.W., Sagoe, S.D., Abu, M., 2024. Predicting irrigation water quality indices in a typical mining dominated area in the Upper West region of Ghana using multiple machine learning techniques. Discover Water 4 (1), 46.

Kowalska, J.B., Nicia, P., Gąsiorek, M., Zadrożny, P., Węgrzyn, M.H., Waroszewski, J., 2022. Are natural or anthropogenic factors influencing potentially toxic elements' enrichment in soils in proglacial zones? An example from Kaffiøyra (Oscar II Land, Spitsbergen). International Journal of Environmental Research and Public Health 19 (20), 13703.

Kuffour, R., Tiimub, M., Manu, I., Owusu, W., 2020. The effect of illegal mining activities on vegetation: a case study of bontefufuo area in the Amansie West District of Ghana. East African Scholars Journal of Agriculture and Life Sciences 3 (11), 353–359. https://doi.org/10.36349/easjals.2020.v03i11.002.

Ma, J., Chen, L., Chen, H., Wu, D., Ye, Z., Zhang, H., Liu, D., 2023. Spatial distribution, sources, and risk assessment of potentially toxic elements in cultivated soils using isotopic tracing techniques and Monte Carlo simulation. Ecotoxicol. Environ. Saf. 259, 115044.

McKone, T.E., Daniels, J.I., 1991. Estimating human exposure through multiple pathways from air, water, and soil. Regul. Toxicol. Pharm. 13 (1), 36–61.

Mensah, A.K., Mahiri, I.O., Owusu, O., Mireku, O.D., Wireko, I., Kissi, E.A., 2015a. Environmental impacts of mining: a study of mining communities in Ghana. Applied Ecology and Environmental Sciences 3 (3), 81–94.

Mensah, N.J., Ayiah-Mensah, F., Sebiawu, G.E., 2015b. Heavy metal characteristics of soils at the Damang-Abosso mining areas of western region Ghana. IJSER 6 (2), 1302–1309.

Müller, G., 1981. Dei Schwermetallbelstung der sedimente des Neckars and seiner Nebenfusse: Eine estandsaufnahme. Chemical Zeitung 105, 157–164.

Nikolaidis, C., Orfanidis, M., Hauri, D., Mylonas, S., Constantinidis, T., 2013. Public health risk assessment associated with heavy metal and arsenic exposure near an abandoned mine (Kirki, Greece). International journal of environmental health research 23 (6), 507–519.

Ofori, S.A., Dwomoh, J., Yeboah, E.O., Martin, A.L., Nti, S., Philip, A., Asante, C., 2024. A ecological study of galamsey activities in Ghana and their physiological toxicity. Asian Journal of Toxicology, Environmental, and Occupational Health 2 (1), 53–72. https://doi.org/10.61511/ajteoh.v2i1.2024.395.

Opoku, P.A., Anornu, G.K., Gibrilla, A., Owusu-Ansah, E.D.G.J., Ganyaglo, S.Y., Egbi, C. D., 2020. Spatial distributions and probabilistic risk assessment of exposure to heavy metals in groundwater in a peri-urban settlement: case study of Atonsu-Kumasi. Ghana. Groundwater for Sustainable Development 10, 100327.
Opoku, R.B., Dankyi, E., Christian, A., Aryeetey, R., 2024. Environmental exposure and potential health impact of heavy metals in previous mining communities in Ghana. Health Sciences Investigations Journal 5 (2), 702–709.
Owusu-Nimo, F., Mantey, J., Nyarko, K.B., Appiah-Effah, E., Aubynn, A., 2018. Spatial distribution patterns of illegal artisanal small scale gold mining (Galamsey) operations in Ghana: A focus on the Western Region. Heliyon 4 (2), e00534. https://doi.org/10.1016/j.heliyon.2018.e00534.
Oze, C., Fendorf, S., Bird, D.K., Coleman, R.G., 2007. Chromium geochemistry of serpentine soils. Int. Geol. Rev. 49 (9), 801–835.
Penteado, J.O., de Lima Brum, R., Ramires, P.F., Garcia, E.M., Dos Santos, M., da Silva Júnior, F.M.R., 2021. Health risk assessment in urban parks soils contaminated by metals, Rio Grande city (Brazil) case study. Ecotoxicology and Environmental Safety, 208, 111737.
Sakyi, P.A., Kwayisi, D., Nunoo, S., Ocran, E., Su, B.X., Malaviarachchi, S.P., 2024. Tectonic Evolution of Alternating Paleoproterozoic Belts and Basins in the Birimian terrane in Southeastern West African Craton. Journal of African Earth Sciences, 105449.
Smedley, P.L., Kinniburgh, D.G., 2002a. A review of the source, behavior, and distribution of arsenic in natural waters. Appl. Geochem. 17 (5), 517–568.
USEPA, 2011. Exposure factors handbook: 2011 edition. National Center for Environmental Assessment, Office of Research and Development, U.S. Environmental Protection Agency. EPA/600/R-09/052F.
Wani, Z.A., Ahmad, Z., Asgher, M., Bhat, J.A., Sharma, M., Kumar, A., Sharma, V., Kumar, A., Pant, S., Lukatkin, A.S., Anjum, N.A., 2023. Phytoremediation of potentially toxic elements: Role, status and concerns. Plants 12 (3), 429.
Weissmannová, H.D., Pavlovský, J., 2017. Indices of soil contamination by heavy metals–methodology of calculation for pollution assessment (minireview). Environ. Monit. Assess. 189 (12), 616.
Wireko-Gyebi, R.S., King, R.S., Braimah, I., Lykke, A.M., 2020. Local Knowledge of Risks associated with Artisanal Small-scale Mining in Ghana. Int. J. Occup. Saf. Ergon. 1–17. https://doi.org/10.1080/10803548.2020.1795374.
Wu, J., Lu, J., Li, L., Min, X., Luo, Y., 2018. Pollution, ecological-health risks, and sources of heavy metals in soil of the northeastern Qinghai-Tibet Plateau. Chemosphere 201, 234–242.
Xu, B., 2011. Clustering educational digital library usage data: Comparisons of latent class analysis and K-Means algorithms. Utah State University.
Zhang, H., Pu, M., Li, H., Lu, B., Zhang, X., Li, S., Zhao, C., Pu, W., Liu, R., Guo, K., Zhang, T., 2024. Progress and prospects for remediation of soil potentially toxic elements pollution: a state-of-the-art review. Environ. Technol. Innov. 103703.
Emmanuel, A.Y., Jerry, C.S., Dzigbodi, D.A., 2018. Review of environmental and health impacts of mining in Ghana. Journal of Health and Pollution 8 (17), 43–52.
Smedley, P.L., Kinniburgh, D.G., 2002b. A review of the source, behaviour and distribution of arsenic in natural waters. Applied Geochemistry 17 (5), 517–568.
Rudnick, R. L.,Gao, S. (2003). Composition of the continental crust. Treatise on Geochemistry, vol. 3. *Treat Geochem*, 1-64.

Further Reading

Amoah, P., Eweje, G., 2022. Barriers to environmental sustainability practices of multinational mining companies in Ghana: an institutional complexity perspective. Corporate Governance: the International Journal of Business in Society 22 (2), 364–384. https://doi.org/10.1108/CG-06-2021-0229.
Arhin, E., Zango, S.M., Berdie, B.S., 2016. Geochemical background of some potentially toxic and essential trace elements in soils at the Nadowli District of the Upper West Region of Ghana. J. Earth Environ. Health Sci. 2 (2), 56–65.
Darko, G., Boakye, K.O., Nkansah, M.A., Gyamfi, O., Ansah, E., Yevugah, L.L., Acheampong, A., Dodd, M., 2019. Human health risk and bioaccessibility of toxic metals in topsoils from Gbani mining community in Ghana. Journal of Health and Pollution, 9(22), p.190602.
Fosu-Mensah, B.Y., Okoffo, E.D., Mensah, M., 2022. Assessment of farmers' knowledge and pesticides management in cocoa production in Ghana. International Journal of Advanced and Applied Sciences 9 (3), 100–110.
Goldfarb, R.J., Groves, D.I., Gardoll, S., 2010. Orogenic gold and geologic time: a global synthesis. Ore Geol. Rev. 38 (1), 1–27.
Kabata-Pendias, A., 2011. Trace Elements in Soils and Plants, (4th ed.). CRC Press.
Mohammed, A.-S., Asumah, M.N., Padhi, B.K., Sinha, A., Mohammed, I., Jamil, S., Boasiako, O.A., Leman, N., Kabir, R., 2023. Predictors of SARS-CoV-2 vaccine uptake among health professionals: a cross-sectional study in Ghana. Vaccines 11 (1), 190. https://doi.org/10.3390/vaccines11010190.
Nesse, W.D., 2013. Introduction to optical mineralogy, (4th ed.). Oxford University Press, New York, p. 121.
Onyeanwuna, U.B., Akakuru, O.C., Opara, A.I., Onyekuru, S.O., Ibeneme, S.I., Ofoh, I.J., Isreal, H., 2024. Application of geological and geo-electric methods in the assessment of corrosivity, competence, and vulnerability of soils around Southeastern Nigeria. International Journal of Physical Sciences 19 (1), 58–79.
Taylor, S.R., McLennan, S.M., 1985. The Continental Crust: Its Composition and Evolution. Blackwell Scientific.
Yidana, S.M., Ophori, D.U., Banoeng-Yakubo, B., 2012. Groundwater quality evaluation in the Afram Plains area of Ghana. Environ. Earth Sci. 67 (3), 783–794. https://doi.org/10.1007/s12665-011-1513-2.
Cobbina, S.J., Duwiejuah, A.B., Quansah, R., Obiri, S., Bakobie, N., 2015. Comparative assessment of heavy metals in drinking water sources in two small-scale mining communities in northern Ghana. International journal of environmental research and public health 12 (9), 10620–10634.
Taylor, S.R., 1964. Abundance of chemical elements in the continental crust: a new table. Geochim. Cosmochim. Acta 28 (8), 1273–1285.
Zhou, L., Ampon-Wireko, S., Xu, X., Quansah, P.E., Larnyo, E., 2022. Media attention and vaccine hesitancy: examining the mediating effects of fear of COVID-19 and the moderating role of Trust in leadership. PLoS One 17 (2), e0263610. https://doi.org/10.1371/journal.pone.0263610.